Limited, Cambs, UK) and stained with hematoxylin–eosin (HE). Slides were then digitized with a graphic analyzer system (Mac Scope ver2.55, Mitsuya shoji, Shiga, Japan). Areas of infarction were measured and infarct volumes were calculated as described above.

Construction and preparation of PTD-FNK, PTD-Bcl-xL and PTD-myc-FNK

An oligonuleotide encoding MGYGRKKRRQRRRG [the human immunodeficiency virus type 1/trans-activator of transcription (TAT) protein transduction domain of 11 amino acids is underlined] was ligated to the 5′-end of the FNK or Bcl-x_L coding sequence by PCR to construct PTD-FNK or PTD-Bcl-x_L, respectively. An oligonucleotide encoding GEQKLISEEDLG (myc TAG sequence is underlined) was inserted between PTD and FNK sequences of PTD-FNK by PCR to obtain PTD-myc-FNK. The ligated DNA fragment was inserted between *Nco* I and *Hind* III sites in pPROEX1 expression vector (Invitrogen Japan K.K., Tokyo, Japan). The integrity of the construct was confirmed by sequencing. The resultant plasmid was introduced into *Escherichia coli* DH5αMCR, followed by isopropyl-β-D-thiogalactopyranoside induction. PTD-FNK or PTD-Bcl-x_L protein was solubilized from inclusion bodies with 7 M urea and 2% sodium dodecyl sulfate in the presence of 0.1 mM dithiothreitol, and then subjected to sodium dodecyl sulfate–polyacrylamide gel electrophoresis to purify further. After the gel was briefly incubated in 1 M KCl to visualize the main bands, a band corresponding to PTD-FNK was cut out. PTD-FNK was electrophoretically extracted from the gel slice in extraction buffer (25 mM Tris, 0.2 M Glycine, and 0.1% sodium dodecyl sulfate) for injection into animals. The concentration of PTD-FNK extracted ranged from 1 to 2 mg/mL. (Asoh *et al.* 2002). The extraction buffer was used as the 'Vehicle'.

Immunohistochemistry

To examine the distribution of FNK delivered into the brain after the administration of FNK fused with PTD-myc (0.25 mg/kg) or vehicle into the tail vein (i.v.), the rats were killed with an overdose of halothane followed by cervical dissection. Brains were removed, fixed with 4% paraformaldehyde in 0.1 M phosphate-buffered saline (PBS, pH 7.4) overnight at 4°C, dehydrated, and routinely embedded in paraffin. Sections were cut 4 μm thick. Immunohistochemistry was performed using the Vectastain ABC elite kit (Vector Laboratories, Burlingame, CA, USA) coupled with the diaminobenzidine reaction, where biotinylated goat anti-rabbit IgG provided in the kit was used as the secondary antibody. Sections were treated with endogenous peroxidase quenching (0.3% H_2O_2 for 10 min) and pre-blocked with serum-free blocking solution (DAKO, Carpinteria, CA, USA) for 30 min prior to incubation with the primary antibody. Rabbit anti-Myc tag polyclonal antibody (1 : 100 dilution, 4°C overnight, Upstate biotechnology, Lake Placid, NY, USA) was employed as the primary antibody. PBS was used instead of the primary antibody or ABC reagent as a negative control. Low-magnification digital images (half-magnification of five fields in the cortex and striatum at each indicated time point were analyzed to determine relative areas occupied by myc immunoreactivity with NIH IMAGE software. The value for brain sections of rats injected with the vehicle was used as the background to be subtracted from that for rats injected with the protein.

Score of neurological deficits

Neurological deficits were scored on a scale of 0–5 as follows (Murakami *et al.* 1998): 0, no neurological deficit; 1, failure to fully extend the right forepaw; 2, circling to the right; 3, falling to the right; 4, unable to walk spontaneously; and 5, dead.

MRI measurements

MRI experiments were performed using an 18-cm bore 7T horizontal magnet (Magnex Scientific, Abingdon, UK) with a Varian Unity-INOVA-300 (Varian Inc., Palo Alto, CA, USA) system equipped with an actively shielded gradient. A 6-cm internal diameter quadrature birdcage coil was used in the study.

A rat anesthetized with halothane (4% for induction, 1% for maintenance) in nitrous oxide/oxygen (70%/30%, v/v) was positioned on its back in a self-made plexiglass stereotaxic holder with its head rigidly held by ear and tooth bars. The axial position of the rat was adjusted until the image slice was 5 mm caudal to the rhinal fissure in the center of the coil.

Cerebral perfusion was measured using continuous spin labeling (Williams *et al.* 1992) with centric-ordered variable-tip-angle gradient echo (VTE-GRE). Adiabatic inversion of inflowing arterial protons was accomplished with an axial gradient of ± 4500 Hz/mm and continuous RF transmission of approximately 600 Hz at a frequency offset of ± 9000 Hz, which placed the inversion plane at ± 20 mm from the imaging plane. Three seconds of inversion were followed by a 100 ms delay in order to eliminate the effect of regional transit time delay (Alsop and Detre 1996). GE parameters were as follows: repetition time/echo time (TR/TE) 5/3 ms; field of view 50 mm × 50 mm; slice thickness 2 mm; matrix size 128 × 64. Forty-eight pairs of images were summed to improve the signal-to-noise ratio.

Magnetization transfer was measured under the same conditions as cerebral perfusion without an axial gradient for adiabatic inversion. T1 was measured using a centric-ordered snapshot-FLASH with a hyperbolic secant inversion pulse (Gowland *et al.* 1989) and 18-point (20–5000 ms) inversion delay. Quantitative cerebral blood flow (CBF) maps were calculated from the cerebral perfusion image, T1 map and magnetization transfer (MTR) map according to the theory described by Ewing *et al.* (2003). Diffusion-weighted imaging was recorded with a Stejskal-Tanner spin-echo sequence with a TE of 40 ms and TR of 2000 ms. Nine coronal slices 2 mm thick were imaged with a field of view of 50 mm × 50 mm and a matrix size of 128 × 128. Diffusion weighting used b-values of 100, 750 and 1500 s/mm^2 to permit calculation of the apparent diffusion coefficient (ADC) map. Three diffusion-weighted imaging measurements with an orthogonal diffusion gradient were performed to calculate the isotropic ADC map. CBF maps and trace ADC maps were computed by MRI image manipulation software (MR vision, MR Vision Co., Menro Park, CA, USA) on a workstation (Blade1000, Sun Microsystems, Milpitas, CA, USA).

In vitro experiments

Neuroblastoma SH-SY5Y cells were cultured in Dulbecco's modified Eagle's medium (Invitrogen Japan K.K.) with 15% fetal bovine serum and penicillin (20 units/mL)-streptomycin (20 μg/mL), and plated onto a 24-well collagen-coated microplate (Iwaki Co., Ltd., Tokyo, Japan) at a density of 1×10^5 cells/cm^2. One day after cultivation, the cells were rinsed with serum-free medium and

pre-treated with 300 pM PTD-FNK (Asoh *et al.* 2002) and/or 100 nM FK506 (Muramoto *et al.* 2003) for 2 h. The cells were then stimulated with 1 μM thapsigargin (TG) (Sigma, St Louis, MO, USA) and incubated for 24 h. Viable cells with polygonal soma were enumerated under a phase-contrast microscope (×200) in five fields per well in three independent experiments.

For the determination of cytosolic-free Ca^{2+}, the fluorescent Ca^{2+} indicator Fluo-3AM (Molecular Probes, Eugene, OR, USA) was added to the medium at a final concentration of 1 μM and incubated for 3 h. Then, the cells were washed once with serum-free Dulbecco's modified Eagle's medium, pre-treated with 300 pM PTD-FNK and/or 100 nM FK506, and further stimulated with 1 μM TG for 2 h. Fluorescence was imaged by confocal scanning laser microscopy (Fluoview FV/300; Olympus, Tokyo, Japan) using excitation and emission filters of 488 and 510 nm, respectively. Fluo-3AM signals were quantified using the NIH IMAGE program.

To investigate the inhibitory effect of FK506 on the incorporation of PTD-FNK, SH-SY5Y cells were cultured on a 4-well plastic dish (SonicSeal Slide; Nalge Nunc International, Rochester, NY, USA) coated with collage type I (Cellmatrix I-P, Nitta Gelatin Inc., Osaka, Japan). One day after cultivation, the cells were rinsed with serum-free medium and treated with 300 pM PTD-FNK and/or 100 nM FK506 for 2 h. The cells were washed with PBS, and fixed with 4% paraformaldehyde in PBS for 20 min. After washing with PBS, the cells were treated with 0.3% Triton, and then incubated in blocking solution (3% bovine serum albumin, 3% goat serum albumin). The cells were treated with a primary anti-$Bclx_L$ monoclonal antibody 35–32 (Asoh *et al.* 2002). Subsequently, the cells were treated with BODIPY FL goat anti-mouse IgG (1 : 500; Molecular Probes Inc.). Finally, the cells were stained with propidium iodide (1 μM) and imaged by confocal scaning lazer microscopy (Fluoview FV/300). Images were analyzed using the NIH IMAGE program to obtain the BODIPY FL fluorescence intensity of each cell.

Statistics

Values are expressed as the mean ± SEM when not indicated. Statistical differences were calculated using one-way analysis of variance (ANOVA) followed by Student–Newman–Keuls test. For non-parametric multi-comparisons, the Steel-Dwass method was used to analyze neurological deficit scores. Data were analyzed with *post hoc* multiple comparisons by the Student–Neuman–Keuls test for *in vitro* experiments.

Results

Transduction of PTD-FNK into neural cells of the brain

At first, we tested the delivery of PTD-FNK protein into neurons of the brain by intravenously (i.v.) injecting Myc-tagged PTD-FNK protein (PTD-Myc-FNK). At 0.5, 1, 3, and 6 h after injection, rat brains were quickly removed for staining with anti-myc antibody. We found strong immunoreactivity in the microvessels as well as the cytoplasm of neurons in the cerebral cortex and striatum, compared with those of a control rat injected with vehicle (Fig. 1). Reactivity peaked at 1 h after injection, gradually decreased with a half-span of 3.6 h, and persisted until 6 h (Fig. 1k and

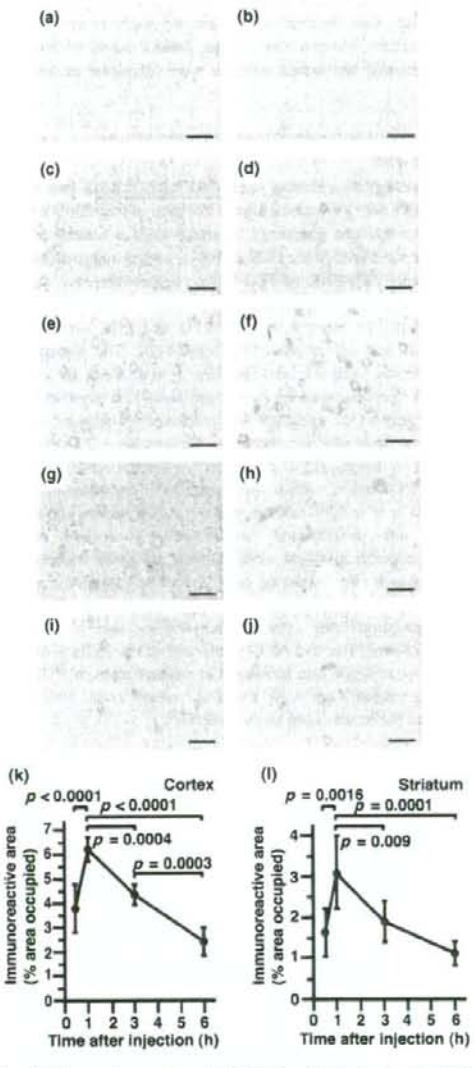

Fig. 1 Delivery of myc-tagged PTD-FNK protein into neurons in the brain. (a–j) Immunohistochemical staining. After injection of vehicle (a and b) or PTD-myc-FNK. (0.25 mg/kg) (c–j) into the tail vein of rats, brains were removed at 0.5 h (c and d), 1 h (e and f), 3 h (g and h), and 6 h (i and j) to prepare paraffin sections. Brain sections were stained with a rabbit anti-MYC polyclonal antibody, coupled with a Vectastain ABC elite kit for the diaminobenzidine reaction. The cerebral cortex (a, c, e, g and i) and striatum (b, d, f, h and j) are shown. Scale bars: 50 μm. (k and l) PTD-myc-FNK remaining in brain tissues was quantified as described in Materials and methods. Data are shown as the means with SD (vertical bars) after statistical analysis by one-way ANOVA.

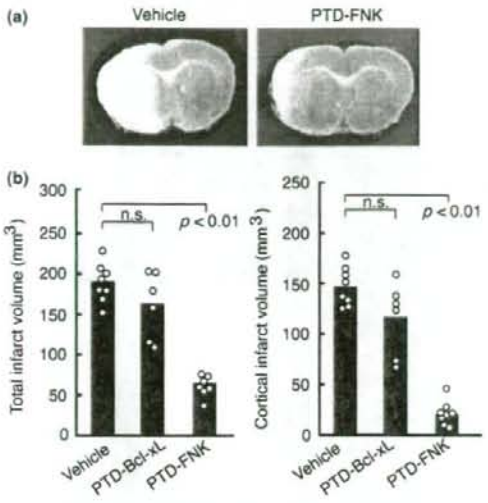

Fig. 2 Effects of pre-treatment with PTD-FNK and PTD-Bcl-x_L on infarct volume. (a) Representative images of brain sections stained with 2,3,5-triphenyletrazolium chloride (TTC). (b) Right panel shows the effects on total infarct volume. Left panel depicts the effects on cortical infarct volume. Vehicle ($n = 8$) or PTD-Bcl-xL (0.5 mg/kg; $n = 6$) or PTD-FNK (0.25 mg/kg; $n = 8$,) was injected intraperitoneally at 3 h before ischemia. Values for individual rats and the average are shown as circles and bars, respectively.

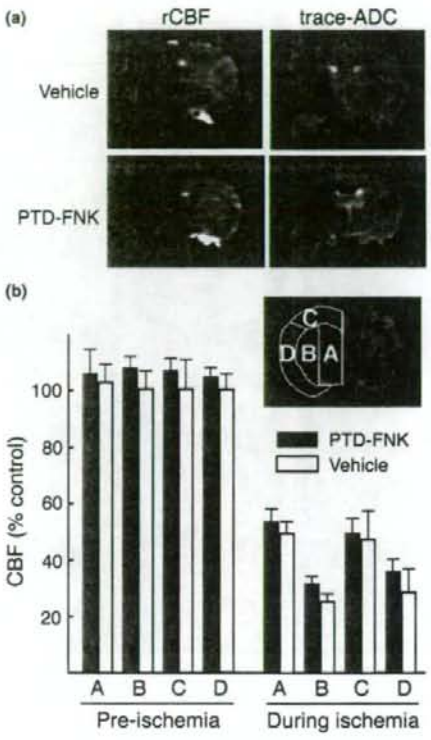

Fig. 3 Effects of PTD-FNK on cerebral blood flow. (a) Representative MRI rCBF and trace ADC images. PTD-FNK or vehicle was administered at 3 h before ischemia. The left side is the ischemic hemisphere. (b) Effects of PTD-FNK on cerebral blood flow. PTD-FNK (0.25 mg/kg) or vehicle was administered at 3 h before ischemia. Cerebral blood flow (CBF) in the area indicated (A, B, C and D in the ischemic hemisphere) of each rat before PTD-FNK or vehicle injection as a control (100%). After injection of PTD-FNK or vehicle, CBF before (pre-ischemia) and during ischemia was measured using MRI perfusion images as described in Materials and methods and expressed as %control. Average values with SD from three independent experiments are shown.

l). The time course of the incorporation was nearly the same as that of *in vitro* experiments (Asoh *et al.* 2002). Thus, these results indicate that PTD-myc-FNK promptly crosses the blood–brain barrier and enters neuronal cells in the rat brain.

Effect of pre-treatment on infarct volume

We examined the effects of pre-treatment with PTD-FNK or PTD-Bcl-x_L delivered by the intraperitoneal route 3 h before initiating focal ischemia. Since the TAT peptide mediates the delivery of proteins by intraperitoneal (i.p.) administration as well as intravenous (i.v.) injection at comparable levels (Cai *et al.* 2006), we used intraperitoneal administration as an easier method in preliminary experiments. Pre-treatment with PTD-FNK (0.25 mg/kg) significantly reduced ischemic damage produced by MCA occlusion, whereas PTD-Bcl-x_L exerted little effect (Fig. 2). Since PTD-FNK was more effective at 0.25 mg/kg than 0.5 or 5 mg/kg for an unknown reason (data not shown), we set the dose of PTD-FNK at 0.25 mg/kg throughout subsequent experiments. Except for in these preliminary experiments, we injected PTD-FNK, PTD-Bcl-x_L and FK506 intravenously throughout this study.

Effect on cerebral blood flow by PTD-FNK

To test the effect of PTD-FNK on CBF before or during ischemia, we measured CBF in certain areas using a magnetic resonance imaging device, an 18-cm bore 7T horizontal magnet with a Varian Unity-INOVA-300 system. Cerebral blood flow was not significantly influenced by PTD-FNK pre-treatment before and during ischemia (Fig. 3b).

In addition, MRI diffusion weighted-images revealed nearly the same extent of reduction of regional CBF (rCBF) and trace-ADC (Fig. 3a). Thus, PTD-FNK transduction did not relieve the ischemic conditions.

Effect of post-treatment with PTD-FNK on infarct volume

For practical application for patients with cerebral infarction, it is necessary to evaluate the effects of post-treatment. Post-

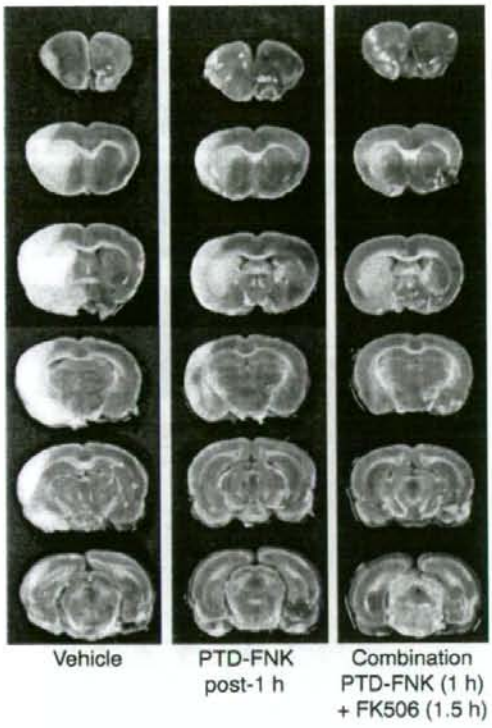

Fig. 4 Representative sections outlining the infarct area in the rat brain subjected to ischemia for 1.5 h, reperfused and stained with 2,3,5-triphenyletrazolium chloride (TTC) after 24 h. (Left) Vehicle-treated rats. (Middle) PTD-FNK (0.25 mg/kg) administered 1 h after initiating ischemia. (Right) Combination of PTD-FNK (0.25 mg/kg) at 1 h and FK506 (1 mg/kg) at 1.5 h after initiating ischemia.

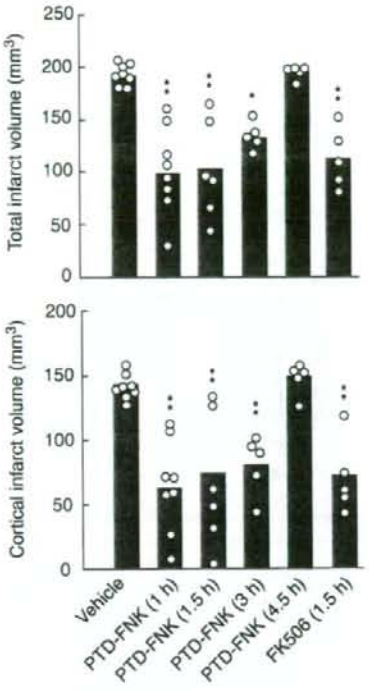

Fig. 5 Effects of post-treatment with PTD-FNK on infarct volume. Upper panel shows the effects on total infract volume. Lower panel depicts the effects on cortical infarct volume. Vehicle ($n = 8$) or PTD-FNK (0.25 mg/kg) was intravenously injected at 1 h ($n = 8$), 1.5 h ($n = 6$), 3 h (1.5 h after reperfusion; $n = 5$), and 4.5 h (3 h after reperfusion; $n = 5$) after ischemia. FK506 (1 mg/kg) was intravenously injected at 1.5 h ($n = 5$). Values for individual rats and the average are shown as circles and bars, respectively. $^{**}p < 0.01$ against vehicle by one-way ANOVA.

treatment with PTD-FNK considerably improved the infarction, with about a 50% reduction in the cortex (Figs. 4 and 5), although this was less than with pre-treatment. The reduction was significant until 3 h after initiating ischemia (1.5 h after reperfusion). The effect of post-treatment with PTD-FNK was comparable to that of a relatively high dose (1 mg/kg) of FK506, whose protective effects were in good agreement with previous reports [Fig. 5, bar FK506 (1.5 h); Sharkey and Butcher 1994; Arii *et al.* 2001].

Effect of combination therapy on infarct volume

Since post-treatment with FK506 improves ischemic injury (Arii *et al.* 2001; Furuichi *et al.* 2003), we applied a combination of PTD-FNK and FK506 as post-treatment. Based on previous studies (Arii *et al.* 2001; Furuichi *et al.* 2003), we chose a dose of 1 mg/kg of FK506 at 1.5 h after ischemia, which was shown to exert neuroprotective activity (Fig. 5). When we administered PTD-FNK and FK506 together at 1.5 h after ischemia, the reduction in infarct volume was less than that by each single injection [cf. PTD-FNK (1.5 h) + FK506 (1.5 h) in Fig. 6 with PTD-FNK (1.5 h) in Fig. 4 or FK506 (1.5 h) in Fig. 5]; however, when post-treatment with PTD-FNK at 1 h after ischemia was followed by FK506 with a 30-min lag period (at 1.5 h), the effect was markedly enhanced (cf. Fig. 5 with Fig. 6). Notably, the average infarct volume in the cortex reached 14% (ranging from 0.8% to 41%) of the vehicle-treated group. The reduction was significant until 4.5 h after initiating ischemia and 3 h reperfusion [PTD-FNK (4.5 h) + FK506 (5 h) in Fig. 6].

Infarct volume at 1 week after ischemia

It is possible that combination therapy delayed the progression of injury but did not improve it. To exclude this

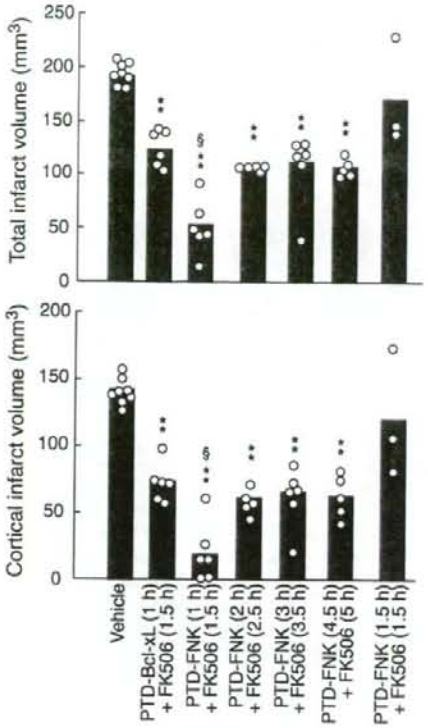

Fig. 6 Efficacy of combination therapy. In combination therapy, PTD-FNK (0.25 mg/kg, i.v.; 1 h, $n = 6$; 2 h, $n = 5$; 3 h, $n = 6$; 4.5 h, $n = 5$) and FK506 (1 mg/kg, i.v.) were injected at the indicated time points (with a 30-min lag period) after initiating ischemia. The combination of PTD-Bcl-x_L (0.5 mg/kg, i.v. at 1 h after ischemia) and FK506 (1 mg/kg, i.v. at 1.5 h after initiating ischemia) [PTD-Bcl-x_L (1 h) + FK506 (1.5 h); $n = 6$] and the combination of PTD-FNK (0.25 mg/kg, i.v.) and FK506 (1 mg/kg, i.v.) at 1.5 h after initiating ischemia without a lag period [PTD-FNK (1.5 h) + FK506 (1.5 h); $n = 3$] were also administered for comparison. Vehicle data from Fig. 5 are re-presented for comparison. Values for individual rats and the average are shown as circles and bars, respectively, as presented in Fig. 5. $^{**}p < 0.01$ against vehicle; $^{\S}p < 0.05$ against the combination of PTD-Bcl-x_L and FK506, by one-way ANOVA.

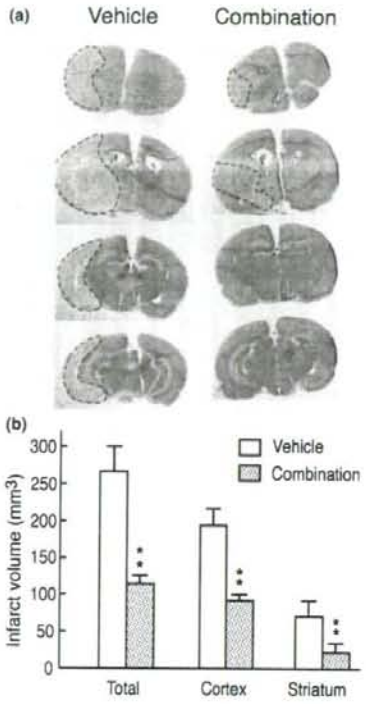

Fig. 7 Time-lag combination therapy reduced the infarct volume even after 1 week. (a) Representative photographs of HE-stained coronal sections of the brain prepared from a rat-treated PTD-FNK (0.25 mg/kg) at 1 h after ischemia and FK506 (1 mg/kg) at 1.5 h after ischemia, at 1 week after 1.5 h of focal ischemia. (b) Effect of combination therapy on total, cortex, and stratum infarct volume. $^{**}p < 0.01$ against vehicle. Six rats in each group.

possibility, we examined whether the protective effects of combination therapy continued for long periods. The protective effects did last for a longer period, for at least 1 week, and resulted in a quite significant reduction of infarct volumes: the infarct volumes fell to 43% (total), 47% (cortex), and 31% (striatum) (Fig. 7). Thus, a single combination treatment markedly improved the infarction. Moreover, it is noteworthy that combination therapy caused a significant reduction of infarct volume even in the striatum ($p < 0.01$), as well as the cortex.

Effect of treatments on edema volume

An increase in edema volume is a hallmark of ischemic infarction. The results of total edema volumes are summarized in Fig. 8. The trend toward a reduction of edema volume was similar to that for total infarct volume. Pre-treatment with PTD-FNK resulted in the lowest edema volume [lane 2: PTD-FNK-0.25 in Fig. 8]. Post-treatment with FNK also had a significant effect until 3 h after ischemia [lane 7: PTD-FNK (3 h) in Fig. 8]. Notably, combination therapy had a significant effect even at 4.5 h after ischemia [lane 14: PTD-FNK (4.5 h) + FK506 (5 h) in Fig. 8]. In this experiment, PTD-Bcl-x_L again showed an insignificant reduction [lane 4: PTD-Bcl-xL-0.5 in Fig. 8].

Effect of treatments on neurological symptom

At 24 h after ischemia, a neurological examination was performed to test actual improvements. Neurological deficits

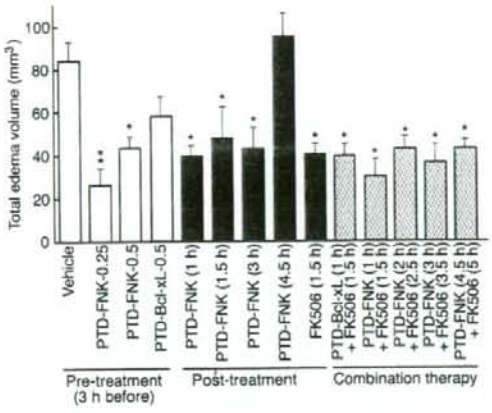

Fig. 8 Effect of therapies on total edema volume after ischemia. Pre-treatment: the vehicle ($n = 8$), PTD-FNK (0.25 or 0.5 mg/kg) (PTD-FNK-0.25; $n = 8$, PTD-FNK-0.5; $n = 8$), or PTD-Bcl-x_L (0.5 mg/kg) (PTD-Bcl-xL-0.5; $n = 6$) was injected 3 h before ischemia. Post-treatment: PTD-FNK (0.25 mg/kg) was injected 1 h [PTD-FNK (1 h); $n = 8$], 1.5 h [PTD-FNK (1.5 h); $n = 6$], 3 h [PTD-FNK (3 h); $n = 5$], or 4.5 h [PTD-FNK (4.5 h); $n = 5$] after initiating ischemia. FK506 was injected 1.5 h after initiating ischemia [FK506 (1.5 h); $n = 5$]. In combination therapy, PTD-Bcl-x_L (0.5 mg/kg) was injected 1 h after initiating ischemia, followed by the injection of FK506 (1 mg/kg) with a 0.5 h time-lag [PTD-Bcl-x_L (1 h) + FK506 (1.5 h); $n = 6$]. PTD-FNK (0.25 mg/kg; 1 h, $n = 6$; 2 h, $n = 5$; 3 h, $n = 6$; 4.5 h, $n = 5$) was injected at the indicated times after ischemia, followed by the injection of FK506 (1 mg/kg) with a 0.5 h time-lag. $^*p < 0.05$; $^{**}p < 0.01$ against vehicle by one-way ANOVA.

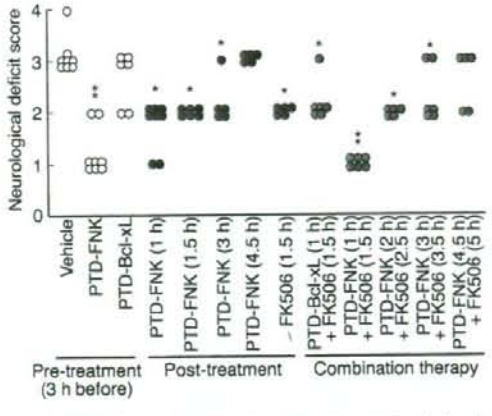

Fig. 9 Effect of therapies on neurological symptoms after ischemia. Pre-treatment: the vehicle ($n = 8$), PTD-FNK (0.25 mg/kg; $n = 8$), or PTD-Bcl-x_L (0.5 mg/kg; $n = 6$) was injected 3 h before ischemia. Post-treatment: PTD-FNK (0.25 mg/kg) was injected 1 h [PTD-FNK (1 h); $n = 8$], 1.5 h [PTD-FNK (1.5 h); $n = 6$], 3 h [PTD-FNK (3 h); $n = 5$], or 4.5 h [PTD-FNK (4.5 h); $n = 5$] after initiating ischemia. FK506 was injected 1.5 h after initiating ischemia [FK506 (1.5 h); $n = 5$]. In combination therapy, PTD-Bcl-x_L (0.5 mg/kg) was injected 1 h after initiating ischemia, followed by FK506 injection (1 mg/kg) with a 0.5 h time-lag [PTD-Bcl-x_L (1 h) + FK506 (1.5 h); $n = 6$]. PTD-FNK (0.25 mg/kg; 1 h, $n = 6$; 2 h, $n = 5$; 3 h, $n = 6$; 4.5 h, $n = 5$) was injected at the indicated times after ischemia, followed by FK506 injection (1 mg/kg) with a 0.5 h time-lag. $^*p < 0.05$; $^{**}p < 0.01$ against vehicle by the Steel-Dwass method.

were scored as described in Materials and methods. The neurological deficit scores were significantly lower in rats pre-treated with PTD-FNK (lane 2: PTD-FNK) than the vehicle (lane 1: Vehicle) or PTD-Bcl-x_L (lane 3: PTD-Bcl-xL) (Fig. 9), showing that a good effect of PTDFNK against ischemic stroke in the reduction of infarct volume accompanied the improvement of neurological symptoms. The improvements in neurological scores with various treatments were in good agreement with the reduction of infarct volumes. Notably, the combination of PTD-FNK at 1 h after ischemia followed by FK506 gave the lowest score in all rats examined [lane 10: PTD-FNK (1 h) + FK506 (1.5 h) in Fig. 9]. All rats were able to walk reasonably smoothly in spite of being unable to fully extend the right forepaw; therefore, the combination therapy was effective not only in reducing infarct volumes but also in improving neurological symptoms. PTD-FNK alone significantly improved scores until 3 h after ischemia [lane 6: PTD-FNK (3 h) in Fig. 9]. Combined therapy also significantly reduced scores until 3 h after ischemia [lane 12: PTD-FNK (3 h) + FK506 (3.5 h) in Fig. 9]. At 4.5 h after ischemia [lane 13: PTD-FNK (4.5 h) + FK506 (5 h) in Fig. 9], the Mann–Whitney test revealed a marginally significant improvement compared to the control ($p < 0.05$).

Effects on physiological variables

Finally, we examined physiological parameters before and during ischemia and after reperfusion (data not shown). Values were considered normal for rectal and head temperature, blood pressure, pCO_2, pO_2, pH and blood glucose in control animals. Although rats in four groups [post-treatment with PTD-FNK: PTD-FNK (1 h) and (1.5 h), PTD-FNK (1 h) + FK506 (1.5 h) and PTD-Bcl-x_L (1 h) + FK506 (1.5 h)] showed slightly higher pCO_2 values (42.8–48.1 mmHg) during ischemia compared with the vehicle group (40.2 mmHg), these differences were not statistically significant. The slight increase in pCO_2 was not the result of PTD-FNK, because pre-and post-administration (1.5 h, 3 h and 4.5 h) of PTD-FNK did not increase pCO_2 values. When arterial pCO_2 rose over 60 mmHg in the MCA occlusion model rat, CBF appeared to be modulated by arterial pCO_2 in an exponential fashion and markedly increased (Jones *et al.* 1989). These small differences in arterial pCO_2 should have little influence on CBF, as shown in Fig. 3. Thus, there were no significant side effects of

PTD-FNK either by itself or in combination with FK506 for physiological parameters.

These results strongly suggest that the neuroprotective effects were not the result of secondary effects such as lowering temperature, but indeed because of PTD-FNK itself and/or the combination with FK506.

In vitro experiments explaining the time-lag effect

The main mechanism underlying neuronal death in stroke and anoxic and traumatic brain damage is excitotoxicity, which is triggered by the excessive activation of ionotropic glutamate receptors, leading to a rapid influx of Ca^{2+} that triggers cell death (Dirnagl *et al.* 1999). Thus, we focused on the movement of calcium ions. To explore the mechanism by which time-lag treatment causes an enhanced effect, we used a human neuroblastoma cell line, SH-SY5Y, in *in vitro* experiments because the protective effect by FK506 was confirmed in SH-SY5Y (Muramoto *et al.* 2003). When cells were treated with TG, which is a potent inhibitor of Ca^{2+}-ATPase (Ca^{2+}-pump), the concentration of cytosolic Ca^{2+} increased. Thus, we monitored cytosolic Ca^{2+} ions using the fluorescence of Fluo-3AM (Fig. 10a–g). Pre-treatment with PTD-FNK suppressed the increase of Ca^{2+} induced by TG, whereas pre-treatment with FK506 did not; however, FK506 inhibited cell death induced by TG (Fig. 10h). Pre-treatment with FK506 and PTD-FNK at the same time increased the Ca^{2+} level and did not suppress cell death (Fig. 10g and h). In contrast, when FK506 was added with a 30-min lag time, the elevation in the Ca^{2+} level was suppressed, and the cytoprotective effect of the combination on cell death was marked. A time-lag of 30 min was sufficient (Fig. 10h, insert); thus, the time-lag effect was evident in this *in vitro* experiment.

Since FK506 has been reported to block endocytosis in cultured cells (Lai *et al.* 2000; Kumashiro *et al.* 2005), FK506 may inhibit the translocation of PTD-FNK into cells when it is administered simultaneously, or before PTD-FNK administration. Indeed, the simultaneous addition of FK506 significantly inhibited the incorporation of PTD-FNK, compared with the addition of PTD-FNK alone (Fig. 10i–m). FK506 did not exhibit a significant inhibitory effect on the incorporation of PTD-FNK when FK506 was added 30 min later (Fig. 10l and m). These findings reasonably explain why a time lag is essential for the administration of FK506 to have a synergistic effect.

Discussion

In this study, we found significant protective effects of PTD-FNK against rat brain focal ischemia, even if it was administrated 3 h after ischemia. More importantly, the combination of PTD-FNK and FK506 showed a striking protective effect when those drugs were given with a 30-min time lag.

To date, the reduction in cortical infarct volume achieved by post-treatment with FK506 has been 50% (Sharkey and Butcher 1994). A marked reduction was achieved in total and cortical infarct volume to 50% and 25%, respectively, by perturbing the interaction between the NMDA receptor and PSD-95 using the protein transduction method at 1h after the onset of ischemia (Aarts *et al.* 2002). The method used in our present study is much more effective and has a longer therapeutic time-window than previous methods. We attained maximum reduction at 1 h after ischemia in the total and cortical infarct volume to 27% and 14%, respectively. Intracerebroventricular administration of a peptide inhibitor of c-Jun N-terminal kinase with the PTD peptide showed strong neuroprotection in a mild ischemia mouse model (Borsello *et al.* 2003). Since the authors obtained the infarct mice by 30-min ischemia and intraventricularly injected the PTD peptide, direct comparison with our results (by 90-min ischemia) may be difficult.

Compared with previous studies using wild-type Bcl-x_L, PTD-FNK alone was more effective at a very low dose, one-thirty-sixth of the dose of PTD-Bcl-x_L used by Cao *et al.* (2002), or one-fourth of the dose of PTD-Bcl-x_L used by Kilic *et al.* (2002). Actually, PTD-Bcl-x_L failed to reduce the infarct volume and edema volumes, and neurological deficit scores as much as PTD-FNK (Figs 2, 6, 8 and 9). In addition, the mole dose used in this study (8 nmole/kg) was significantly lower than that for peptide transduction by Aarts *et al.* 2002 (20 mmole/kg) or by Borsello *et al.* 2003 (~11 mg/kg, or ~4 μmole/kg). The lower dose is reasonably expected to reduce the possibility of side effects of the protein transduction peptide.

When treatment with PTD-FNK was followed by an injection of FK506 with a 30-min lag time, the cytoprotective effects were markedly enhanced in terms of the decrease of infarct volume and extension of the time window. It is essential for clinical treatments to extend the time window of treatment after the onset of ischemia because it takes considerable time to initiate clinical treatments. In this study, we succeeded in extending the period to 4.5 h after ischemia, which could be sufficient to begin to treat emergency cases of cerebral infarction in a hospital. It was reported that FK506 and Bcl-x_L suppress the activation of matrix metalloproteinase-9 (Oliver *et al.* 2000; Migita *et al.* 2006), which enhances cerebral edema by blood–brain barrier disruption (Gasche *et al.* 2001). Therefore, the possibility remains that the combination with PTD-FNK and FK506 showed a significant reduction of brain edema through protection of the blood brain barrier.

The improvement obtained by combination therapy is because of a protective effect but not due to a delay in the progression of injury (Fig. 7). Our own previous study (Arii *et al.* 2001) and Sharkey and Butcher (Sharkey and Butcher 1994) failed to show a protective effect on the striatum by FK506 in the same filament MCA occlusion model. Inter-

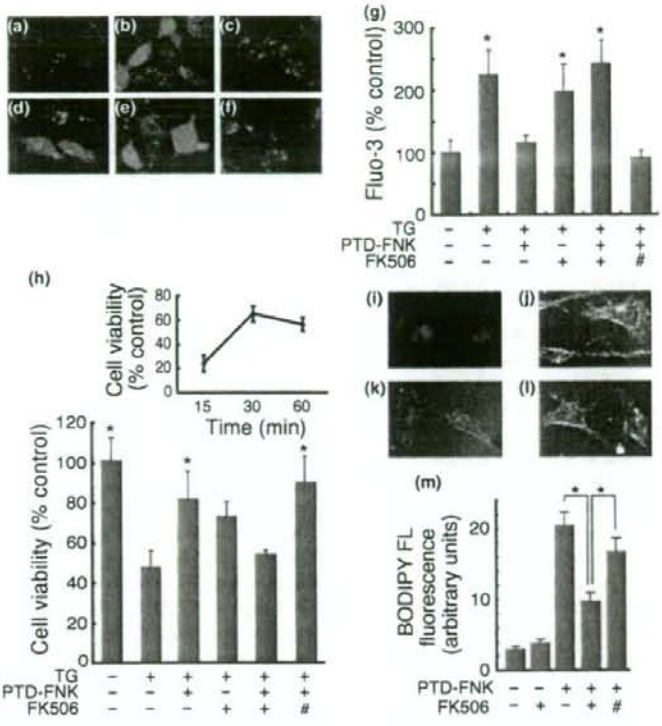

Fig. 10 Time-lag treatment of PTD-FNK with FK506 in cultured cells. (a–f) Two hours before stimulation with thapsigargin (TG) (1 μM), SH-SY5Y neuroblastoma cells were pre-treated with PTD-FNK (300 pM) and/or FK506 (100 nM). Representative images with confocal scanning microscopy are shown (a–f). (a): control, (b): TG, (c): PTD-FNK + TG, (d): FK506 + TG, (e): PTD-FNK + FK506 (simultaneously) + TG, (f): PTD-FNK + FK506 (30-min time lag) + TG. (g) For each experimental group, 20 cells were analyzed with the NIH IMAGE program to quantify Fluo-3 signals. Data are % intensity of Fluo-3 AM in the normal group (no exposure to PTD-FNK, FK506 and TG), and expressed as the mean with SEM. #, 30 min after pre-treatment with PTD-FNK, FK506 was added. *$p < 0.05$ against the normal group using *post hoc* multiple comparisons with the Student–Neuman–Keuls test. (h) Protective effects of PTD-FNK and FK506 against TG-induced SH-SY5Y cell death. Two hours before stimulation with TG (1 μM), cells were pre-treated with PTD-FNK (300 pM) and/or FK506 (100 nM), as described above. After incubation for 1 day, viable cells (five fields in each well, four wells in each experimental group) were counted. Cells not stimulated with TG were used as a control (100%). Data are expressed as the mean with SEM. #, 30 min after pre-treatment with PTD-FNK, FK506 was added. *$p < 0.05$ against cells treated only with TG using *post hoc* multiple comparisons with the Student–Neuman–Keuls test. The insert shows the protective effects against TG when FK506 was added at the indicated time after pre-treatment with PTD-FNK. (i–m) Inhibitory effect of FK506 on internalization of PTD-FNK. SH-SY5Y cells were treated with PTD-FNK (350 nM) and/or FK506 (100 nM) for 2 h, as described above. After incubation, the cells were subjected to immunostaining using anti-Bcl-x antibody (primary antibody) and secondary antibody (BODIPY FL). The cells were co-stained with propidium iodide. Representative images with confocal scanning microscopy are shown (i–l). (i): FK506, (j): PTD-FNK, (k): PTD-FNK + FK506 (simultaneous), (l) PTD-FNK + FK506 (30-min time lag). (m) After imaging by confocal laser scanning microscopy, 40 cells from each experimental group were analyzed with the NIH IMAGE program to obtain BODIPY FL fluorescence intensity. Data are expressed as the mean with SEM. #, 30 min after pre-treatment with PTD-FNK, FK506 was added. *$p < 0.001$ by ANOVA.

estingly, we found a reduction of infarct volume in the striatum after 1 week (68%, Fig. 7). This protective effect on the striatum must be due to the combination of the two drugs and the timing of administration. Thus, this combination could be a practical treatment for cerebral infarction. The procedure also significantly improved the neurological symptoms accompanied by a reduction of infarct volume.

It was reported that FK506 blocks endocytosis (Lai *et al.* 2000; Kumashiro *et al.* 2005). We indeed showed inhibition of the transduction of PTD-FNK by FK506, which explained

why a lag time is essential for the administration of FK506 in combination therapy.

Moreover, to explore the mechanisms of how PTD-FNK synergistically protects with FK506, we performed an *in vitro* study measuring the cytosolic calcium concentration. The combination of PTD-FNK with FK506 provided a cytoprotective effect against an increase in cytosolic Ca^{2+} only when cells were treated with PTD-FNK followed by FK506 with a 30-min lag time. An important cellular target of FK506 is the ubiquitous FK506-binding protein, FKBP12, a 12-kDa member of the immunophilin family (Marks 1996). FKBP12 is physiologically associated with the ryanodine receptor (RyR) and 1,4,5-triphosphate receptor (IP_3R), which release Ca^{2+} into cytosol (Jayaraman *et al.* 1992; Cameron *et al.* 1995). Whereas FK506 stimulates the binding of FKBP12 to calcineurin, it causes a dissociation of FKBP12 from RyR, or IP_3 receptors. When FKBP12 is stripped from those receptors, the calcium channel becomes 'leaky', leading to enhanced calcium release upon stimulation (Marks 1997). Thus, a high dose of FK506 exerts multiple effects on intracellular Ca^{2+} homeostasis (Bultynck *et al.* 2003), and inhibits the sarcoplasmic/endoplasmic reticulum Ca^{2+}-Mg^{2+}-ATPase, Ca^{2+} pump, leading to an increase in the cytosolic Ca^{2+} concentration (Bultynck *et al.* 2000).

In this study, we showed an increase in the cytosolic Ca^{2+} concentration after FK506 treatment with TG. Since a higher cytosolic Ca^{2+} concentration should be toxic to cells (Paschen and Doutheil 1999), the protective effect of FK506 could involve other mechanisms independent of Ca^{2+}. In contrast, Bcl-2, or probably Bcl-x_L, can inhibit the release of calcium from endoplasmic reticulum (Nutt *et al.* 2002; Breckenridge *et al.* 2003). In fact, we showed that PTD-FNK decreased the fluorescent intensity of Fluo-3AM after exposure to TG. When PTD-FNK was added with FK506 with no time-lag, the effect of FK506 to increase the cytosolic Ca^{2+} level overcame that of PTD-FNK. When PTD-FNK was followed by FK506 with a lag-time, the effect of PTD-FNK to decrease the cytosolic Ca^{2+} level overcame that of FK506. Thus, combined treatment may evoke independent cytoprotective activities of FK506 and PTD-FNK without inducing a toxic effect by FK506. PTD-FNK treatment may have two major protective effects if combined with FK506 treatment; its own protective effect and a reduction of various adverse effects of FK506 treatment, such as an increase in the cytosolic Ca^{2+} level.

Understanding the molecular mechanism of the combined effects may help us to develop more effective therapies for cerebral infarction; however, our procedure improves neurological symptoms and reduces the infarct volume in stroke rats to the maximum level even 4.5 h after ischemia. Furthermore, if FK506, which is now under clinical trials in the USA for stroke therapy, is combined with PTD-FNK, the protective effect is significantly increased and the adverse effect of FK506 could be reduced. Further studies are necessary to show clinical usefulness; however, this combination therapy could become a promising method of tackling cerebral infarction.

References

Aarts M., Liu Y., Liu L., Besshoh S., Arundine M., Gurd J. W., Wang Y. T., Salter M. W. and Tymianski M. (2002) Treatment of ischemic brain damage by perturbing NMDA receptor-PSD-95 protein interactions. *Science* **298**, 846–850.

Alsop D. C. and Detre J. A. (1996) Reduced transit-time sensitivity in noninvasive magnetic resonance imaging of human cerebral blood flow. *J. Cereb. Blood Flow Metab.* **16**, 1236–1249.

Arakawa M., Yasutake M., Miyamoto M., Takano T., Asoh S. and Ohta S. (2007) Transduction of anti-cell death protein FNK protects isolated rat hearts from myocardial infarction induced by ischemia/reperfusion. *Life Sci.* **80**, 2076–2084.

Arii T., Kamiya T., Arii K., Ueda M., Nito C., Katsura K. I. and Katayama Y. (2001) Neuroprotective effect of immunosuppressant FK506 in transient focal ischemia in rat: therapeutic time window for FK506 in transient focal ischemia. *Neurol. Res.* **23**, 755–760.

Asoh S., Ohtsu T. and Ohta S. (2000) The super anti-apoptotic factor Bcl-xFNK constructed by disturbing intramolecular polar interactions in rat Bcl-x_L. *J. Biol. Chem.* **275**, 37240–37245.

Asoh S., Ohsawa I., Mori T., Katsura K., Hiraide T., Katayama Y., Kimura M., Ozaki D., Yamagata K. and Ohta S. (2002) Protection against ischemic brain injury by protein therapeutics. *Proc. Natl Acad. Sci. USA* **99**, 17107–17112.

Asoh S., Mori T., Nagai S., Yamagata K., Nishimaki K., Miyato Y., Shidara Y. and Ohta S. (2005) Zonal necrosis prevented by transduction of the artificial anti-death FNK protein. *Cell Death Differ.* **12**, 384–394.

Borsello T., Clarke P. G. H., Hirt L., Vercelli A., Repici M., Schorderet D. F., Bogousslavsky J. and Bonny C. (2003) A peptide inhibitor of c-Jun N-terminal kinase protects against excitotoxicity and cerebral ischemia. *Nat. Med.* **9**, 1180–1186.

Breckenridge D. G., Germain M., Mathai J. P., Nguyen M. and Shore G. C. (2003) Regulation of apoptosis by endoplasmic reticulum pathways. *Oncogene* **22**, 8608–8618.

Bultynck G., De Smet P., Weidema A. F., Ver Heyen M., Maes K., Callewaert G., Missiaen L., Parys J. B. and De Smedt H. (2000) Effects of the immunosuppressant FK506 on intracellular Ca^{2+} release and Ca^{2+} accumulation mechanisms. *J. Physiol.* **525**, 681–693.

Bultynck G., Sienaert I., Parys J. B., Callewaert G., De Smedt H., Boens N., Dehaen W. and Missiaen L. (2003) Pharmacology of inositol trisphosphate receptors. *Pflugers Arch.* **445**, 629–642.

Cai S. R., Xu G., Becker-Hapak M., Ma M., Dowdy S. F. and McLeod H. L. (2006) The kinetics and tissue distribution of protein transduction in mice. *Eur. J. Pharm. Sci.* **27**, 311–319.

Cameron A. M., Steiner J. P., Sabatini D. M., Kaplin A. I., Walensky L. D. and Snyder S. H. (1995) Immunophilin FK506 binding protein associated with inositol 1,4,5-trisphosphate receptor modulates calcium flux. *Proc. Natl Acad. Sci. USA* **92**, 1784–1788.

Cao G., Pei W., Ge H. *et al.* (2002) In Vivo delivery of a Bcl-xL fusion protein containing the TAT protein transduction domain protects against ischemic brain injury and neuronal apoptosis. *J. Neurosci.* **22**, 5423–5431.

Chen H., Zhang L., Jin Z., Jin E., Fujiwara M., Ghazizadeh M., Asoh S., Ohta S. and Kawanami O. (2007) Anti-apoptotic PTD-FNK protein suppresses lipopolysaccharide-induced acute lung injury in rats. *Exp. Mol. Pathol.* **83**, 377–384.

Denicourt C. and Dowdy S. F. (2003) Protein transduction technology offers novel therapeutic approach for brain ischemia. *Trends Pharmacol. Sci.* **24**, 216–218.

Dirnagl U., Iadecola C. and Moskowitz M. A. (1999) Pathobiology of ischaemic stroke: an integrated view. *Trends Neurosci.* **22**, 391–397.

Drake M., Friberg H., Boris-Möller F., Sakata K. and Wieloch T. (1996) The immunosuppressant FK506 ameliorates ischemic damage in the rat brain. *Acta Physiol. Scand.* **158**, 155–159.

Ewing J. R., Wei L., Knight R. A., Pawa S., Nagaraja T. N., Brusca T., Divine G. W. and Fenstermacher J. D. (2003) Direct comparison of local cerebral blood flow rates measured by MRI arterial spin-tagging and quantitative autoradiography in a rat model of experimental cerebral ischemia. *J. Cereb. Blood Flow Metab.* **23**, 198–209.

Furuichi Y., Katsuta K., Maeda M., Ueyama N., Moriguchi A., Matsuoka N., Goto T. and Yanagihara T. (2003) Neuroprotective action of tacrolimus (FK506) in focal and global cerebral ischemia in rodents: dose dependency, therapeutic time window and long-term efficacy. *Brain Res.* **965**, 137–145.

Garcia-Criado F. J., Palma-Vargas J. M., Valdunciel-Garcia J. J., Toledo A. H., Misawa K., Gomez-Alonso A. and Toledo-Pereyra L. H. (1997) Tacrolimus (FK506) down-regulates free radical tissue levels, serum cytokines, and neutrophil infiltration after severe liver ischemia. *Transplantation* **64**, 594–598.

Gasche Y., Copin J. C., Sugawara T., Fujimura M. and Chan P. H. (2001) Matrix metalloproteinase inhibition prevents oxidative stress-associated blood-brain barrier disruption after transient focal cerebral ischemia. *J. Cereb. Blood Flow Metab.* **21**, 1393–1400.

Gold B. G., Storm-Dickerson T. and Austin D. R. (1994) The immunosuppressant FK506 increases functional recovery and nerve regeneration following peripheral nerve injury. *Restor. Neurol. Neurosci.* **6**, 287–296.

Gowland P. A., Leach M. O. and Sharp J. C. (1989) The use of an improved inversion pulse with the spin-echo/inversion-recovery sequence to give increased accuracy and reduced imaging time for T1 measurements. *Magn. Reson. Med.* **12**, 261–267.

vander Heiden M. G. and Thompson C. B. (1999) Bcl-2 proteins: regulators of apoptosis or of mitochondrial homeostasis? *Nat. Cell Biol.* **1**, E209–E216.

Ide T., Morikawa E. and Kirino T. (1996) An immunosuppressant, FK506, protects hippocampal neurons from forebrain ischemia in the mongolian gerbil. *Neurosci. Lett.* **204**, 157–160.

Jayaraman T., Brillantes A. M., Timerman A. P., Fleischer S., Erdjument-Bromage H., Tempst P. and Marks A. R. (1992) FK506 binding protein associated with the calcium release channel (ryanodine receptor). *J. Biol. Chem.* **267**, 9474–9477.

Jones S. C., Bose B., Furlan A. J., Friel H. T., Easley K. A., Meredith M. P. and Little J. R. (1989) CO_2 reactivity and heterogeneity of cerebral blood flow in ischemic, border zone, and normal cortex. *Am. J. Physiol.* **257**, H473–H482.

Kashio A., Sakamoto T., Suzukawa K., Asoh S., Ohta S. and Yamasoba T. (2007) A protein derived from the fusion of TAT peptide and FNK, a Bcl-x(L) derivative, prevents cochlear hair cell death from aminoglycoside ototoxicity in vivo. *J. Neurosci. Res.* **85**, 1403–1412.

Katsura K., Kurihara J., Hiraide T., Takahashi K., Kato H. and Katayama Y. (2003) Effects of FK506 on the translocation of protein kinase C and CaM kinase II in the gerbil hippocampal CA1 neurons. *Neurol. Res.* **25**, 522–527.

de Keyser J., Sulter G. and Luiten P. G. (1999) Clinical trials with neuroprotective drugs in acute ischaemic stroke: are we doing the right thing? *Trends Neurosci.* **22**, 535–540.

Kilic E., Dietz G. P., Hermann D. M. and Bähr M. (2002) Intravenous TAT-Bcl-X_L is protective after middle cerebral artery occlusion in mice. *Ann. Neurol.* **52**, 617–622.

Kumashiro S., Lu Y. F., Tomizawa K., Matsushita M., Wei F. Y. and Matsui H. (2005) Regulation of synaptic vesicle recycling by calcineurin in different vesicle pools. *Neurosci. Res.* **51**, 435–443.

Kuroda S. and Siesjö B. K. (1996) Postischemic administration of FK506 reduces infarctvolume following transient focal brain ischemia. *Neurosci. Res. Commun.* **19**, 83–90.

Lai M. M., Luo H. R., Burnett P. E., Hong J. J. and Snyder S. H. (2000) The calcineurin-binding protein cain is a negative regulator of synaptic vesicle endocytosis. *J. Biol. Chem.* **275**, 34017–34020.

Lyons W. E., George E. B., Dawson T. M., Steiner J. P. and Snyder S. H. (1994) Immunosuppressant FK506 promotes neurite outgrowth in cultures of PC12 cells and sensory ganglia. *Proc. Natl Acad. Sci. USA* **91**, 3191–3195.

Marks A. R. (1996) Cellular functions of immunophilins. *Physiol. Rev.* **76**, 631–649.

Marks A. R. (1997) Intracellular calcium-release channels: regulators of cell life and death. *Am. J. Physiol.* **272**, H597–H605.

Matsuda T., Yamaguchi Y., Matsumura F. *et al.* (1998) Immunosuppressants decrease neutrophil chemoattractant and attenuate ischemia/reperfusion injury of the liver in rats. *J. Trauma* **44**, 475–484.

Migita K., Maeda Y., Abiru S. *et al.* (2006) Immunosuppressant FK506 inhibits matrix metalloproteinase-9 induction in TNF-alpha-stimulated human hepatic stellate cells. *Life Sci.* **78**, 2510–2515.

Ministry of Health, Labour and Welfare, Japan (2002) Health and Sanitation, in Statistical abstract on health and welfare in Japan (Ministry of Health, Labour and Welfare, Japan, ed) pp. 69–130. Health and Welfare Statistics Association of Japan, Tokyo.

Murakami K., Kondo T., Kawase M., Li Y., Sato S., Chen S. F. and Chan P. H. (1998) Mitochondrial susceptibility to oxidative stress exacerbates cerebral infarction that follows permanent focal cerebral ischemia in mutant mice with manganese superoxide dismutase deficiency. *J. Neurosci.* **18**, 205–213.

Muramoto M., Yamazaki T., Nishimura S. and Kita Y. (2003) Detailed in vitro pharmacological analysis of FK506-induced neuroprotection. *Neuropharmacology* **45**, 394–403.

Nakashima-Kamimura N., Nishimaki K., Mori T., Asoh S. and Ohta S. (2008) Prevention of chemotherapy-induced alopecia by the anti-death FNK protein. *Life Sci.* **82**, 218–225.

Nishinaka Y., Sugiyama S., Yokota M., Saito H. and Ozawa T. (1993) Protective effect of FK506 on ischemia/reperfusion-induced myocardial damage in canine heart. *J. Cardiovasc. Pharmac.* **21**, 448–454.

Nutt L. K., Pataer A., Pahler J., Fang B., Roth J. A., McConkey D. J. and Swisher S. G. (2002) Bax and Bak promote apoptosis by modulating endoplasmic reticular and mitochondrial Ca^{2+} stores. *J. Biol. Chem.* **277**, 9219–9225.

Ohsawa I., Ishikawa M., Takahashi K., Watanabe M., Nishimaki K., Yamagata K., Katsura K.-I., Katayama Y., Asoh S. and Ohta S. (2007) Hydrogen acts as a therapeutic antioxidant by selectively reducing cytotoxic oxygen radicals. *Nat. Med.* **13**, 688–694.

Oliver L., Tremblais K., Guriec N., Martin S., Meflah K., Menanteau J. and Vllette F. M. (2000) Influence of bcl-2-related proteins on matrix metalloproteinase expression in a rat glioma cell line. *Biochem. Biophys. Res. Commun.* **273**, 411–416.

Ozaki D., Sudo K., Asoh S., Yamagata K., Ito H. and Ohta S. (2004) Transduction of anti-apoptotic proteins into chondrocytes in cartilage slice culture. *Biochem. Biophys. Res. Commun.* **313**, 522–527.

Paschen W. and Doutheil J. (1999) Disturbances of the functioning of endoplasmic reticulum: a key mechanism underlying neuronal cell injury? *J. Cereb. Blood Flow Metab.* **19**, 1–18.

Reed J. C. (1997) Double identity for proteins of the Bcl-2 family. *Nature* **387**, 773–776.

Sakr M., Zetti G., MaClain C., Gavaler J., Nalesnik M., Todo S., Starzl T. and Van Thiel D. (1992) The protective effect of FK506 pretreatment against renal ischemia/reperfusion injury in rats. *Transplantation* **53**, 987–991.

Schwarze S. R., Ho A., Vocero-Akbani A. and Dowdy S. F. (1999) *In vivo* protein transduction: delivery of a biologically active protein into the mouse. *Science* **285**, 1569–1572.

Sharkey J. and Butcher S. P. (1994) Immunophilins mediate the neuroprotective effects of FK506 in focal cerebral ischaemia. *Nature* **371**, 336–339.

Sudo K., Asoh S., Ohsawa I., Ozaki D., Yamagata K., Ito H. and Ohta S. (2005) The anti-cell death FNK protein protects cells from death induced by freezing and thawing. *Biochem. Biophys. Res. Commun.* **330**, 850–856.

Swanson R. A., Morton M. T., Tsao-Wu G., Savalos R. A., Davidson C. and Sharp F. R. (1990) A semiautomated method for measuring brain infarct volume. *J. Cereb. Blood Flow Metab.* **10**, 290–293.

Tara S., Miyamoto M., Asoh S., Ishii N., Yasutake M., Takagi G., Takano T. and Ohta S. (2007) Transduction of the anti-apoptotic PTD-FNK protein improves the efficiency of transplantation of bone marrow mononuclear cells. *J. Mol. Cell. Cardiol.* **42**, 489–497.

Wadia J. S. and Dowdy S. F. (2002) Protein transduction technology. *Curr. Opin. Biothechnol.* **13**, 52–56.

Warlow C. P. (1998) Epidemiology of stroke. *Lancet* **352**, 1–4.

Williams D. S., Detre J. A., Leigh J. S. and Koretsky A. P. (1992) Magnetic resonance imaging of perfusion using spin inversion of arterial water. *Proc. Natl Acad. Sci. USA* **89**, 212–216.

Yagita Y., Kitagawa K., Matsushita K., Taguchi A., Mabuchi T., Ohtsuki T., Yanagihara T. and Matsumoto M. (1996) Effect of immunosuppressant FK506 on ischemia-induced degeneration of hippocampal neurons in gerbils. *Life Sci.* **59**, 1643–1650.

Available online at www.sciencedirect.com
ScienceDirect
Life Sciences 82 (2008) 218 – 225
Life Sciences
www.elsevier.com/locate/lifescie

Prevention of chemotherapy-induced alopecia by the anti-death FNK protein

Naomi Nakashima-Kamimura [a], Kiyomi Nishimaki [a], Takashi Mori [b], Sadamitsu Asoh [a], Shigeo Ohta [a,*]

[a] *Department of Biochemistry and Cell Biology, Institute of Development and Aging Sciences, Graduate School of Medicine, Nippon Medical School, Kawasaki-city, Kanagawa, 211-8533, Japan*

[b] *Institute of Medical Science, Department of Pathology, Saitama Medical Center/University, Kawagoe, Saitama, 350-8550, Japan*

Received 12 September 2007; accepted 6 November 2007

Abstract

Many anticancer drugs attack rapidly dividing cells, including not only malignant cells but also hair follicle cells, and induce alopecia. Chemotherapy-induced alopecia (CIA) is an emotionally distressing side effect of cancer chemotherapy. There is currently no useful preventive therapy for CIA. We have previously constructed anti-death rFNK protein from rat Bcl-x_L by site-directed mutagenesis to strengthen cytoprotective activity. When fused to the protein transduction domain (PTD) of HIV/Tat, the fusion protein PTD (TAT)-rFNK successfully entered cells from the outside in vitro and in vivo to exhibit anti-death activity against apoptosis and necrosis. Here, we show that topical application of FNK protected against CIA in a newborn rat model. The protective activity against hair-loss was observed in 30–1000 nM TAT-rFNK administrative groups in a dose-dependent manner. Furthermore, a human version of FNK (hFNK) fused to other PTD peptides exhibited a protective ability. These results suggest that PTD-FNK possesses protective activity against CIA and is not restricted to a sequence of PTD peptides or species of FNK. Thus, PTD-FNK represents potential to develop a useful method for preventing CIA in cancer patients.

Keywords: Alopecia; Hair loss; Cell death; Bcl-x_L; Protein therapy; Protein transduction domain

Introduction

Chemotherapy-induced alopecia (CIA) is one of the most common and psychologically distressing side effects of cancer chemotherapy. Although many methods have been proposed for decades, progress has been insufficient for the prevention or treatment. Many anti-cancer drugs induce apoptosis in hair follicles and cause hair loss (Schilli et al., 1998; Botchkarev et al., 2000; Selleri et al., 2004; Hendrix et al., 2005; Kim et al., 2006). Although the underlying molecular mechanism(s) of the hair follicle apoptosis induced by chemotherapy is poorly understood, the p53, Fas and *c*-kit signaling pathways were recently shown to be involved in apoptosis (Botchkarev et al., 2000; Sharov et al., 2003, 2004). On the other hand, a wide variety of agents have been reported to exhibit a protective effect on CIA in various rodent models, including 1, 25-dihydroxyvitamin D_3 (Jimenez and Yunis, 1992b), a bacteria-derived biologic response modifier ImuVert (Hussein et al., 1990), an anti-oxidant *N*-acetylcysteine (D'Agostini et al., 1998), a combination of ImuVert and *N*-acetylcysteine (Jimenez et al., 1992a), a cytokine interleukin 1 (Hussein, 1991; Jimenez et al., 1992b), an immunosuppressant cyclosporine A (Paus et al., 1994; Hussein et al., 1995), a hypertrichotic agent minoxidil (Hussein, 1995), a monoclonal antibody against doxorubicin (Balsari et al., 1994), a soybean-derived immunostimulating peptide soymetide-4 (Tsuruki et al., 2005), an α-lactalbumin-derived immunostimulating peptide Gly-Leu-Phe (Tsuruki and Yoshikawa, 2005), an immunomodulator AS101 (Sredni et al., 1996), a FPRL1 receptor agonist peptide MMK-1 (Tsuruki and Yoshikawa, 2006), an apoptosis inhibitor M50054 (2,2'-methylenebis) (Tsuda et al., 2001), prostaglandins (Malkinson et al., 1993), epidermal, fibroblast and keratinocyte growth factors (Jimenez and Yunis, 1992a; Braun et al., 2006), and a segment polarity gene product sonic hedgehog (Sato et al.,

* Corresponding author. Tel.: +81 44 733 9267; fax: +81 44 733 9268.
E-mail address: ohta@nms.ac.jp (S. Ohta).

0024-3205/$ - see front matter © 2007 Elsevier Inc. All rights reserved.
doi:10.1016/j.lfs.2007.11.011

2001), although not all are reported to have anti-apoptotic activity. It is likely that hair loss is caused by not only apoptosis but also other mechanism(s).

Green et al. and Frankel et al. found that the transcriptional activator of transcription (TAT) protein from human immunodeficiency virus-1 (HIV-1) possesses a unique ability to enter cells from the extracellular environment (Green and Loewenstein, 1988; Frankel and Pabo, 1988). The domain that mediates the translocation of the protein was identified 11 amino acid residues, and termed protein transduction domain (PTD) or cell-penetrating peptide (CPP). We have previously made anti-death rFNK protein, which was constructed from rat Bcl-x_L by site-directed mutagenesis (Y22*F*/Q26*N*/R165*K*) to strengthen cytoprotective activity (Asoh et al., 2000), and fused to the protein transduction domain (PTD) of HIV-1/Tat protein (Asoh et al., 2002; Snyder and Dowdy, 2005), and showed that PTD (TAT)-rFNK rapidly entered cultured cells or reached chondrocytes in slice cultures of cartilage when added into culture media (Asoh et al., 2000, 2002; Ozaki et al., 2004; Asoh et al., 2005) and was delivered into the liver and brain when injected i.p. into mice (Asoh et al., 2002, 2005). In our previous studies, TAT-rFNK successfully protected chondrocytes from death induced by NO and anti-Fas antibody (Ozaki et al., 2004), reduced ischemic injury (Asoh et al., 2002; Nagai et al., 2007; Arakawa et al., 2007), mitigated carbon tetrachloride-induced liver injury (Asoh et al., 2005), protected cells from death induced by freezing and thawing (Sudo et al., 2005) and aminoglycoside toxicity (Kashio et al., 2007), and improved the transplantation efficiency of bone marrow mononuclear cells (Tara et al., 2007). Lately we found that TAT-rFNK prevented necrosis and acute hepatic injury with zonal death induced by carbon tetrachloride. It suggests that TAT-rFNK protects against cell death from both apoptosis and necrosis, and has great potential for clinical applications to prevent cell death (Asoh et al., 2005).

Here, we show that the topical application of rFNK significantly protected hair follicle cells from CIA in a newborn rat model. The protective activity against hair loss was observed in TAT-rFNK administrative groups in a dose-dependent manner. Furthermore, a human version of FNK (hFNK) was also examined, where hFNK was fused with various peptides carrying protein-transduction activity (TAT, R9, K2R7, and R7G6). All these proteins exhibited protection activity against CIA.

Materials and methods

CIA model

Wistar rats (10 day-old) were purchased from Nippon SLC (Hamamatsu, Shizuoka, Japan). Rats were fed ad libitum and housed under a 12-hour light cycle. Alopecia was induced by intraperitoneal injection of etoposide (3 mg/kg, a single treatment) on rat pups (13 day-old). Animal protocols were approved by the Animal Care and Use Committee of Nippon Medical School.

Chemicals

Etoposide was purchased from Sigma (Sigma-Aldrich Japan, Tokyo, Japan) and dissolved in dimethyl sulfoxide (DMSO) at the concentration of 20 mg/ml and further diluted with saline (Otsuka Normal Saline, Otsuka Pharmaceutical Co.-Ltd., Tokyo, Japan) at use.

Construction of human FNK

Five amino acid residues are different between human and rat Bcl-x_L proteins, as follows: Gly (human) and Glu (rat) at residues 40, Ser (human) and Pro (rat) at residues 43, Met (human) and Arg (rat) at residues 45, Ala (human) and Ser (rat) at residues 168, and Glu (human) and Asp (rat) at residues 193 (GeneBank Accession No. L20121 for human Bcl-x_L and Accession No. U72350 for rat Bcl-x_L). To construct a human FNK version, pEF1BOS ratFNK (Asoh et al., 2000), in which ratFNK was inserted at the Xba I site of pEF1BOS, was used as a template for PCR-based site-directed mutagenesis. PCR was independently performed to obtain four PCR products using following four primer pairs: the first is a pair of 5'-primer EF1α-2 (5'-GGGGTTTTATGCGATG-GAGT-3'; the nucleotide sequence of the vector upstream of the FNK coding region) and 3'-primer 3970 (5'-TTCcGaTT-CAGTgcCTTCTGGGGCTTCAGTC-3'; the codons underlined produce P43S and E40G substitutions) to produce fragment 1, the second is a pair of 5'-primer 3971 (5'-GgcACTGAAtCgGAAAtGGAGACCCCCAGTGC: the codons underlined produce E40G, P43S, and R45M substitutions and the 5'-end half is complementary to the 5'-end half of the primer 3970) and 3'-primer 3974 (5'-GATCCAggcTG-CAATCTTACTCACCAA-3'; the codon underlined produces S168A substitution) to produce fragment 2, the third is a pair of 5'-primer 3973 (5'-GATTGCAgccTGGATGGCCACC-TACCTG-3'; the codon underlined produces S168A substitution, and the 5'-end half is complementary to the 5'-end half of primer 3974) and 3'-end primer 3975 (5'-CCCGTA-GAGtTCCACAAAAGTGTCCCAG-3'; the codon underlined produces D193E substitution) to produce fragment 3, and the fourth is a pair of 5'-primer 3976 (5'-GTGGAaCTCTACGG-GAACAATGCA-3'; the codon underlined produces D193E substitution, and the 5'-end half is complementary to the 5'-end half of primer 3975) and 3'-primer 3932 (5'-GATGGG-GAACACTGCTGTTTA-3'; the nucleotide sequence of the vector downstream of the FNK coding region) to produce fragment 4. Fragments 1 and 2 were mixed and annealed to synthesize the complementary strand, followed by amplification using 5'-primer EF1α-2 and 3'-primer 3974 to produce fragment 1/2. Fragments 3 and 4 were also mixed and annealed to synthesize the complementary strand, followed by amplification using 5'-primer 3973 and 3'-primer 3032 to produce fragment 3/4. Fragments 1/2 and 3/4 were mixed and annealed to synthesize the complementary strand, followed by amplification using 5'-primer EF1α-2 and 3'-primer 3032 to produce a full length of the human FNK coding sequence. After the final PCR product was cloned into the Xba I site of

the vector pEF1BOS, the human FNK coding region was confirmed by DNA sequencing.

Construction of TAT, R9, K2R7, and R7G6-fused hFNK

A DNA sequence encoding TAT-fused hFNK (Table 1) was constructed by the exactly same method for constructing that of TAT-rFNK DNA (Asoh et al., 2002) and cloned between the Nde I and Hind III sites of *E. coli* expression vector pET-21a (Novagen, Madison, WI) to obtain pET-21a-TAT-hFNK. To construct R9, K2R7, and R7G6-fused hFNK (Table 1), oligonucleotides encoding R9, K2R7, and R7G6 peptides were ligated at the 5'-end of the coding region of FNK by the one-step PCR method described by Imai et al. (1991), using pET-21a-TAT-hFNK as a template. In brief, primers are designed in inverted tail-to-tail directions to amplify the whole plasmid. PCR was carried out using PfuTurbo DNA polymerase (Stratagene, Garden Grove, CA). The blunt-ended PCR fragment obtained was phosphorylated, self-ligated and used to transform *E. coli*-competent cells. Plasmid DNAs were sequenced to confirm the desired plasmids. The primers were designed as follows: (the nucleotide sequences encoding PTD are underlined). A pair of primers, 5'-GTCGTCGTCGTCGTTCTCAGAGCAACCGGGAGCTG-3' and 5'-GACGACGACGACGCATATGTATATCTCCTTCT-TAAAGTT-3' was used for R9-hFNK. A pair of primers, 5'-TAAACGTAGACGCTCTCAGAGCAACCGGGAGCTG-3' and 5'-CGACGTTTACGACGCATATGTATATCTCCTTCT-TAAAGTTA-3' was used for K2R7-hFNK. A pair of primers, 5'-AGGTCGTGGACGTGGTCGTTCTCAGAGCAACCGG-GAGCTG-3' and 5'-CTACCACGTCCACGACCACGCA-TATGTATATCTCCTTCTTAAAGTTA-3' was used for R7G6-hFNK.

Preparation of PTD-FNKs

PTD-FNK proteins were prepared as described previously (Asoh et al., 2002). In brief, the proteins overexpressed in *E. coli* cells were recovered as inclusion bodies. After solubilization in a buffer containing urea and SDS, the proteins were subjected to SDS-PAGE to remove endotoxin and contaminated proteins. After a band containing PTD-FNK was cut out, PTD-FNK proteins were electrophoretically extracted from the gel slice in extraction buffer (25 mM Tris/0.2 M glycine/0.1% SDS). The extracted protein was used for injection into animals. The extraction buffer was used as a control (vehicle).

Table 1
Sequences of PTD used in this study

Name	Sequence
TAT-rFNK	MGYGRKKRRQRRRGMSQSNRE....
TAT-hFNK	MGYGRKKRRQRRRGMSQSNRE....
R9-hFNK	MRRRRRRRRRSQSNRE....
K2R7-hFNK	MRRKRRKRRRSQSNRE....
R7G6-hFNK	MRGRGRGRGRGRGRSQSNRE....

The amino acid sequences of the N-terminus part of PTD-FNK used in this study are indicated. PTD sequences are underlined.

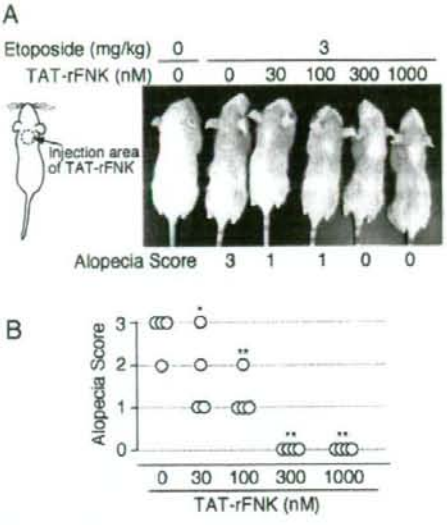

Fig. 1. TAT-rFNK prevents alopecia in a neonatal rat model in a dose-dependent manner. Rat pups (13 days old) were pre-treated by subcutaneous injection of TAT-rFNK (100 μl) at a concentration of 0 (vehicle), 30, 100, 300, and 1000 nM (n=4 each group) into the posterior neck (indicated by arrow) 1 h before intraperitoneal injection of etoposide (3 mg/kg). Alopecia was assessed after 8 days. (A) Representative pups of each group are shown with alopecia score. (B) Alopecia scores of individual pups in each group are shown. *, $P<0.05$; **, $P<0.005$, compared with 0 nM by one-way ANOVA.

Topical application of PTD-FNK

PTD-FNK (100 μl at a concentration of 30 to 1000 nM) or vehicle (25 mM Tris/0.2 M glycine/0.1% SDS buffer used for the PTD-FNK extraction) was subcutaneously (s.c.) injected into the posterior neck before and/or after etoposide injection. Eight days after etoposide injection, the effects of PTD-FNK on alopecia were assessed by examining the degree of hair loss in the area where PTD-FNK was injected, and were scored according to the following scale (Alopecia Score) (Hussein et al., 1995): 0, no detectable alopecia; 1, mild alopecia with less than 50% hair loss; 2, moderately severe alopecia with more than 50% hair loss; 3, severe and total alopecia (see Figs. 1 and 2).

H&E staining

Skin sections (around 5 mm wide × 10 mm along the long axis of the body) where PTD-FNK was injected were removed and fixed with 4% paraformaldehyde in PBS at room temperature. The tissues were dehydrated, embedded in paraffin, longitudinally sectioned with 4 μm in thickness, and stained with hematoxylin and eosin (H&E) for histopathological analysis.

Image analysis of hair follicles

Quantification was performed on H&E-stained skin sections. Images were acquired as digitized tagged-image format files to

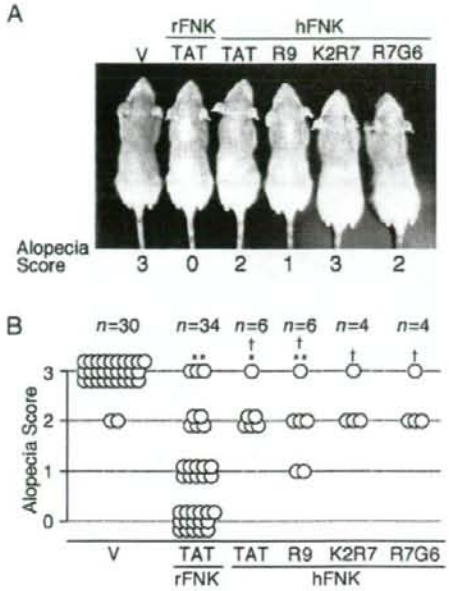

Fig. 2. Human version of FNK fused with various PTD prevented alopecia. Rat pups (13 days old) were pre-treated by subcutaneous injection of vehicle (V) or various PTD-FNK (TAT-rFNK, TAT-hFNK, R9-hFNK, K2R7-hFNK and R7G6-hFNK: 100 μl at 300 nM) into the posterior neck 1 h before intraperitoneal injection of etoposide (3 mg/kg). Alopecia was assessed after 8 days. Note that data of vehicle and TAT-rFNK groups consist of the results of all experiments with the same dose performed in this study. (A) Representative pups of each group are shown with alopecia score. (B) Alopecia scores of individual pups in each group are shown. *, $P<0.05$; **, $P<0.005$, and †, $P<0.005$, compared with Vehicle and TAT-rFNK, respectively, by one-way ANOVA.

retain maximum resolution using an Olympus BX60 microscope with an attached digital camera system (DP-70, Olympus, Tokyo, Japan), and digital images were routed into a Windows PC for quantitative analyses using SimplePCI software (Compix, Inc. Imaging Systems, Cranberry Township, PA). All images (610,200 pixels per field) were captured via an objective lens (×10) and were manually edited to eliminate artifacts. Hair follicle-area is presented as the percentage of manually traced hair follicle pixels divided by the full skin area pixels. Each analysis was performed in a blinded manner by a single investigator.

Results

TAT-rFNK prevents alopecia in a dose-dependent manner

It is well known that etoposide (three times treatments of 1.5 mg/kg/day) induce whole body alopecia in 1 week after the first treatment in a neonatal rat and the model is widely used in CIA studies (Wang et al., 2006). We first examined whether a single treatment of etoposide induces alopecia in order to establish a single-etoposide-treatment protocol to analyze the timing, dose and frequency of TAT-rFNK administration against each etoposide-treatment. We examined the effect of a single treatment of etoposide at a dose of 0.38, 0.75, 1.5, 3 or 6 mg/kg. Rat pups treated with etoposide at a dose of 3 or 6 mg/kg had severe alopecia, starting over the head backwards to the upper half of the back (Fig. 1) or to the entire back (data not shown), respectively, 8 days after etoposide injection. It took 4 weeks for the pups to totally recover from alopecia. On the other hand, rat pups treated with etoposide at a dose of 1.5, 0.75 or 0.38 mg/kg had mild or no detectable alopecia (data not shown). Although we failed to make whole body alopecia, the partial alopecia was useful for our study since our application was topical. We decided to use etoposide at a dose of 3 mg/kg to induce alopecia in further studies.

TAT-rFNK was pre-injected into the posterior neck to assess protective activity against etoposide-induced alopecia (Fig. 1). TAT-rFNK at 30 nM reduced hair loss in the injected area to some extent, and the protective effect on alopecia increased in a dose-dependent manner. There was no difference in the protective effect between the injection of TAT-rFNK at a concentration of 300 nM and 1000 nM.

Various constructs of PTD-FNK prevent alopecia

We compared the alopecia-protective effect between rat and human versions of FNK. rFNK was constructed from rat Bcl-x_L based on the fine 3-dimensional structure (Aritomi et al., 1997; Asoh et al., 2000), where 3 amino acid substitutions (Y22F, Q26N, and R165K) were introduced to abolish 3 hydrogen bonds which stabilize the putative pore-forming domain (α5–α6). These 3 amino acid residues, Y22, Q26, and R165, are conserved in human Bcl-x_L, but 5 amino acid residues at positions 40, 43, 45, 168, and 193 are different between human (Boise et al., 1993) and rat (Shiraiwa et al., 1996) Bcl-x_L amino acid sequences. To examine whether the human version of FNK, hFNK, also exhibited protective activity against etoposide-induced alopecia, we constructed TAT-hFNK as described in Materials and methods. In the TAT-rFNK-injection group, three quarters of pups (Scores 0 and 1, 26 out of 34) were significantly protected from alopecia (Fig. 2). In contrast, most pups in the TAT-hFNK-injection group were significantly protected from alopecia, compared with those in the vehicle (PTD-FNK extraction buffer; 25 mM Tris/0.2 M glycine/0.1% SDS)-injection group, but to a significantly lesser extent, compared with those in the TAT-rFNK-injection group. The rat version of FNK seems to have stronger activity to protect pups from hair loss than the human version.

In the experiments shown above, we used TAT as PTD to deliver FNK into cells. To exclude the possibility that TAT peptide itself has protective activity against etoposide-induced alopecia, hFNK was fused with other peptides which are known or expected to have protein transduction activity. Many studies showed that polyarginine is efficient at entering cells (Wender et al., 2000; Mitchell et al., 2000; Futaki et al., 2001; Suzuki et al., 2002; Park et al., 2002b). hFNK was fused with a 9-mer of arginine (R9), or its modified peptides K2R7 and R7G6 (Table 1), and examined for activity to protect pups from etoposide-induced alopecia (Fig. 2). K2R7-hFNK and R7G6-hFNK

exhibited protective activity to the same extent as TAT-hFNK. Interestingly, two out of 6 pups in the R9-hFNK-injection group obtained the lowest score, Score 1, suggesting that R9-hFNK exhibits stronger activity than TAT-, K2R7- or R7G6-hFNK. R9 peptide appears to more efficiently deliver hFNK into cells than TAT peptide. These results indicate that FNK, irrespective of the human or rat version, itself protects pups from hair loss induced by etoposide.

Pre-injection of TAT-rFNK is most effective to prevent alopecia

To examine the timing and frequency of TAT-rFNK administration for effective protection, the protein was multiply injected at various timings (Fig. 3). In pre-injection groups (Fig. 3, a to f), pups were significantly protected from hair loss to the same extent, irrespective of injection frequency ($P<0.05$ by one-way ANOVA, when the pre-injection group combined with groups a to f was compared with the vehicle group and the simultaneous/post-injection group was combined with groups g to i). Simultaneous injection of TAT-rFNK with etoposide, followed by 3 consecutive daily injections, also protected a single pup from hair loss, but was obviously less effective compared with the pre-injection groups (Fig. 3, g). The pups of post-injection groups (Fig. 3, h and i) were not protected from hair loss. Taken together, TAT-rFNK injection, prior to etoposide administration, is important to exhibit protective activity but the injection frequency is not.

TAT-rFNK prevents hair follicle regression and increases dermal thickness and anagen duration

Effects of TAT-rFNK on alopecia were histopathologically analyzed by H&E staining. Etoposide injection caused shortened hair follicles and decreased number of hair follicles

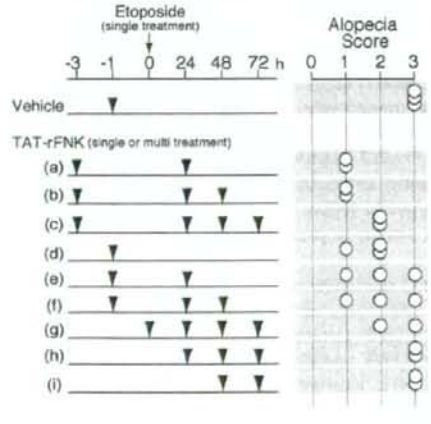

Fig. 3. Effects of TAT-rFNK on alopecia in various regimens. Rat pups (13 days old) received a single or multiple subcutaneous injection of TAT-rFNK (100 μl at 300 nM/shot) into the posterior neck at times indicated by arrowheads. Etoposide (3 mg/kg) was injected at time 0. Alopecia was assessed after 8 days. Alopecia scores of individual pups in each group are shown. Vehicle: $n=3$, (a), (b), (c), (g), (h) and (i): $n=2$, (d), (e) and (f): $n=3$.

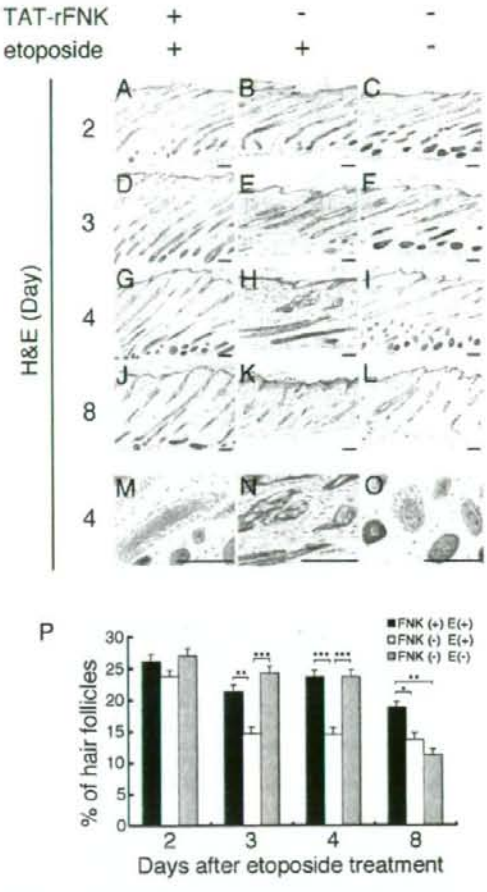

Fig. 4. TAT-rFNK protects follicle cells. 13-day-old rats were pre-treated by s.c. injection of 300 nM TAT-rFNK or vehicle 1 h before etoposide or vehicle i.p. injection (3 mg/kg). (A–L) Representative skin sections stained with H&E on days 2, 3, 4 and 8 after etoposide- and TAT-rFNK-treatments. Scale bars; 100 μm. (M–O) Magnified figures of H&E-stained skin sections on day 4 after etoposide- and TAT-rFNK-treatments. Scale bars; 100 μm. (P) The percentage of hair follicles in TAT-rFNK- and etoposide-treated group (closed bars), in vehicle and etoposide-treated group (open bars) and in vehicle-treated group (semi-closed bars) was analyzed as described in Materials and methods section. Data are expressed as mean ± SEM (vertical bars). Statistical analysis was performed using one-way ANOVA. *, $P<0.01$, **, $P<0.001$, ***, $P<0.0001$.

in the dermis on days 3 and 4, compared with no injection of etoposide (saline containing 2.7% DMSO was injected) (Fig. 4E versus F, H versus I). In contrast, numerous and active hair follicles (the anagen phase of hair cycle) are observed in the dermis on days 3 and 4 in the TAT-rFNK-treated group, which is similar to group with no etoposide, showing the protective effect on chemotherapy-induced alopecia (Fig. 4D versus F and G versus I). On day 4 after treatment with etoposide, some atypical hair shafts caused by the abnormal keratinization were observed in the superficial dermis (Fig. 4H and N). The concentric layer structure composed of outer and inner root

sheaths was disrupted in etoposide-treated group (Fig. 4N), whereas the structure in the TAT-rFNK-treated group was retained like the structure in non-etoposide-treated group (Fig. 4M and O). Many hair follicles were consisted of larger hair bulbs, internal root sheaths (cuticle, Huxley's layer, and Henle's layer), and thicker outer root sheaths, indicating that TAT-rFNK protects hair follicle structure. Next, we quantified the percentage of hair follicle in the skin as described in Materials and methods section. On days 3 and 4, the percentage of hair follicle decreased significantly in etoposide-treatment group but not in TAT-rFNK-treated group (Fig. 4P). In addition, termination of the active phase of hair growth during the first postnatal hair cycle (reflected by the decrease in hair follicles and skin thickness) was detected in the non-etoposide-treated group on day 8 but not in TAT-rFNK-treated group, indicating a delay of termination of anagen phase of hair cycle by TAT-rFNK-treatment (Fig. 4J versus L and P). These data suggest that TAT-rFNK protects hair follicle cells from cell death even at the time hair follicle starts to die to proceed its hair cycle to catagen.

Discussion

In this study, we demonstrated that topical administration of PTD-FNK prevents hair follicle dystrophy induced by etoposide, resulting in very good local protection against alopecia, using the neonatal rat model (Hussein, 1993; Wang et al., 2006). This CIA model was first introduced by Hussein et al. (Hussein et al., 1990; Hussein, 1993). CIA occurs when hair follicles are in the anagen phase (Hussein, 1993) and about 90–95% of hair follicles in the human scalp are in the anagen (Jankovic and Jankovic, 1998). On the other hand, only 10% of hair follicles in adult mice or rats are in the anagen (Chase, 1954). Hussein et al. showed that neonatal rats were useful to mimic the human situation because they have spontaneous anagen hair growth (Hussein et al., 1990; Hussein, 1993). It is therefore easy to assess the effects of CIA and they are commonly used in CIA studies (Wang et al., 2006). We modified this protocol and performed a single-etoposide treatment instead of multi (three times)-etoposide treatments to analyze the timing of TAT-rFNK administration against the etoposide treatment. In our model, we found that PTD-FNK significantly protected hair follicle cells from CIA. The dose of TAT-rFNK was quite low and 100 μl at 300 nM (around 50 μg/kg) was enough to obtain the maximum effect. The human version of FNK also exhibited protective activity against CIA, although the activity was apparently lower than that of the rat version of FNK.

Etoposide is an efficient inducer of apoptosis (Sordet et al., 2003) and causes severe alopecia (Hesketh et al., 2004). Etoposide targets topoisomerase II (topo II), which is a nuclear enzyme to control DNA topology and plays a crucial role in the separation of catenated daughter chromatids produced by DNA replication (Holm, 1994). Recently, etoposide, as well as arsenic trioxide and staurosporine, was proposed to cause topo I-mediated DNA damage by inducing the generation of reactive oxygen species (ROS) from mitochondria (Sordet et al., 2004). In the previous study, we have shown that overexpression of FNK protects cells from apoptosis induced by various cell cycle inhibitors, camptothecin (TN-16, hydroxyurea, and trichostatin A), oxidative stress (hydrogen peroxide and paraquat), and staurosporine, more potently than Bcl-x_L (Asoh et al., 2000). In cells, FNK localizes to mitochondria (Asoh et al., 2002) and functions to maintain intracellular calcium homeostasis (Asoh et al., 2002) and mitochondrial membrane potential (Asoh et al., 2005). It is very likely that FNK prevents etoposide-induced apoptosis, resulting in the protection of hair follicles from alopecia.

A wide variety of agents have been reported to exhibit a protective effect on CIA, but the mechanism(s) of how various agents protect hair follicles from alopecia induced by chemotherapy is poorly characterized. ImuVert (Hussein et al., 1990), interleukin 1 (Hussein, 1991), and 1,25-dihydroxyvitamin D_3 (Jimenez and Yunis, 1992b) could inhibit alopecia induced by cytosine arabinoside and doxorubicin, cytosine arabinoside, and cytoxan, etoposide and adriamycin, respectively, but could not inhibit alopecia induced by cyclophosphamide (Hussein et al., 1990; Hussein, 1991; Paus et al., 1996). On the other hand, cyclosporin A inhibited alopecia induced by cyclophosphamide, etoposide and cytosine arabinoside (Hussein et al., 1995). Similarly, *N*-acetylcysteine inhibited alopecia induced by cyclophosphamide (Jimenez et al., 1992a) and doxorubicin (D'Agostini et al., 1998). These studies clearly indicate a distinction among the agents, regarding the ability to inhibit alopecia. It is very likely that the protection mechanisms are probably different as are the mechanisms of alopecia induced by chemotherapy (Hussein et al., 1995). As discussed above, TAT-rFNK retains the mitochondrial membrane potential (Asoh et al., 2005) and protects cells from cell death induced by a variety of death stimuli in vitro and in vivo (Asoh et al., 2000, 2002; Ozaki et al., 2004; Asoh et al., 2005; Sudo et al., 2005; Nagai et al., 2007; Tara et al., 2007), suggesting that TAT-rFNK protects against chemotherapy-induced alopecia by other anticancer drugs. TAT-rFNK reduced other side effects caused by 5-fluorouarcil, cisplatin, and irinotecan (Watanabe, K. et al., manuscript in preparation).

It has been known for a long time that polybasic peptides like poly-lysine facilitate transduction of proteins into cells in vitro (Ryser, 1968). A number of the other basic peptides, virus- or homeodomain-derived peptides have also been shown for their ability of transduction and known as protein transduction domain (PTD), although the mechanism of their transduction is still unclear (Dietz and Bahr, 2004; Chauhan et al., 2007). Using these PTDs, various kinds of physiologically active proteins have successfully delivered into cells in vitro. The efficient delivery of PTD-fusion proteins in vivo has also been reported. It is considered that PTD-fusion proteins have great potential for therapeutic applications. However, it still remains a challenge to deliver the PTD-fusion proteins to desired targets in vivo because of low protein transduction efficiency and lack of target specific delivery. We have made TAT-fusion rFNK and showed that it reached chondrocytes in slice cultures of cartilage when added into culture media (Ozaki et al., 2004) and was delivered into the liver and brain when injected i.p. into mice (Asoh et al., 2002, 2005). Furthermore, Park et al. showed the penetration of

TAT-SOD (superoxide dismutase) and 9Lys-SOD into the epidermis and the dermis by immunohistochemistry and specific enzyme activities when sprayed on shaved mice skin (Park et al., 2002a). These results suggest that PTD-FNK could penetrate the dermis and epidermis and enter cells. In fact, PTD-FNK protected alopecia and retained hair follicle structure, suggesting that PTD-FNK penetrates epidermis and reaches dermis hair follicle.

Alopecia caused by chemotherapy is irreversible and hair regrowth after chemotherapy can take 3~6 months, although a small percentage of patients fail to completely recover (Veach and Schein, 1997). In CIA, "protein therapy" has advantages over "gene therapy", which inserts a gene into the body and keeps making protein. As PTD-FNK s.c. injected is expected to enter cells located just around the injection point, it provides PTD-FNK at the right time in the right place, thus, PTD-FNK is expected to provide useful technology for protein therapeutics against CIA.

Acknowledgements

This study was supported by grants from the Ministry of Education, Culture, Sports, Science and Technology of Japan (to S.A. and S.O.).

References

Arakawa, M., Yasutake, M., Asoh, S., Miyamoto, M., Takano, T., Ohta, S., 2007. Transduction of anti-cell death protein FNK protects isolated rat hearts from myocardial infarction induced by ischemia/reperfusion. Life Sciences 80 (22), 2076–2084.

Aritomi, M., Kunishima, N., Inohara, N., Ishibashi, Y., Ohta, S., Morikawa, K., 1997. Crystal structure of rat Bcl-x_L. Implications for the function of the Bcl-2 protein family. The Journal of Biological Chemistry 272 (44), 27886–27892.

Asoh, S., Ohtsu, T., Ohta, S., 2000. The super anti-apoptotic factor Bcl-xFNK constructed by disturbing intramolecular polar interactions in rat Bcl-x_L. The Journal of Biological Chemistry 275 (47), 37240–37245.

Asoh, S., Ohsawa, I., Mori, T., Katsura, K., Hiraide, T., Katayama, Y., Kimura, M., Ozaki, D., Yamagata, K., Ohta, S., 2002. Protection against ischemic brain injury by protein therapeutics. Proceeding of the National Academy of Sciences of the United States of America 99 (26), 17107–17112.

Asoh, S., Mori, T., Nagai, S., Yamagata, K., Nishimaki, K., Miyato, Y., Shidara, Y., Ohta, S., 2005. Zonal necrosis prevented by transduction of the artificial anti-death FNK protein. Cell Death and Differentiation 12 (4), 384–394.

Balsari, A.L., Morelli, D., Menard, S., Veronesi, U., Colnaghi, M.I., 1994. Protection against doxorubicin-induced alopecia in rats by liposome-entrapped monoclonal antibodies. The FASEB Journal 8 (2), 226–230.

Boise, L.H., Gonzalez-Garcia, M., Postema, C.E., Ding, L., Lindsten, T., Turka, L.A., Mao, X., Nunez, G., Thompson, C.B., 1993. bcl-x, a bcl-2-related gene that functions as a dominant regulator of apoptotic cell death. Cell 74 (4), 597–608.

Botchkarev, V.A., Komarova, E.A., Siebenhaar, F., Botchkareva, N.V., Komarov, P.G., Maurer, M., Gilchrest, B.A., Gudkov, A.V., 2000. p53 is essential for chemotherapy-induced hair loss. Cancer Research 60 (18), 5002–5006.

Braun, S., Krampert, M., Bodo, E., Kumin, A., Born-Berclaz, C., Paus, R., Werner, S., 2006. Keratinocyte growth factor protects epidermis and hair follicles from cell death induced by UV irradiation, chemotherapeutic or cytotoxic agents. Journal of Cell Science 119 (Pt 23), 4841–4849.

Chase, H.B., 1954. Growth of the hair. Physiological Reviews 34 (1), 113–126.

Chauhan, A., Tikoo, A., Kapur, A.K., Singh, M., 2007. The taming of the cell penetrating domain of the HIV Tat: myths and realities. Journal of Controlled Release 117 (2), 148–162.

D'Agostini, F., Bagnasco, M., Giunciuglio, D., Albini, A., De Flora, S., 1998. Inhibition by oral *N*-acetylcysteine of doxorubicin-induced clastogenicity and alopecia, and prevention of primary tumors and lung micrometastases in mice. International Journal of Oncology 13 (2), 217–224.

Dietz, G.P., Bahr, M., 2004. Delivery of bioactive molecules into the cell: the Trojan horse approach. Molecular and Cellular Neurosciences 27 (2), 85–131.

Frankel, A.D., Pabo, C.O., 1988. Cellular uptake of the tat protein from human immunodeficiency virus. Cell 55 (6), 1189–1193.

Futaki, S., Suzuki, T., Ohashi, W., Yagami, T., Tanaka, S., Ueda, K., Sugiura, Y., 2001. Arginine-rich peptides. An abundant source of membrane-permeable peptides having potential as carriers for intracellular protein delivery. The Journal of Biological Chemistry 276 (8), 5836–5840.

Green, M., Loewenstein, P.M., 1988. Autonomous functional domains of chemically synthesized human immunodeficiency virus tat trans-activator protein. Cell 55 (6), 1179–1188.

Hendrix, S., Handjiski, B., Peters, E.M., Paus, R., 2005. A guide to assessing damage response pathways of the hair follicle: lessons from cyclophosphamide-induced alopecia in mice. The Journal of Investigative Dermatology 125 (1), 42–51.

Hesketh, P.J., Batchelor, D., Golant, M., Lyman, G.H., Rhodes, N., Yardley, D., 2004. Chemotherapy-induced alopecia: psychosocial impact and therapeutic approaches. Supportive Care in Cancer 12 (8), 543–549.

Holm, C., 1994. Coming undone: how to untangle a chromosome. Cell 77 (7), 955–957.

Hussein, A.M., 1991. Interleukin 1 protects against 1-beta-D-arabinofuranosylcytosine-induced alopecia in the newborn rat animal model. Cancer Research 51 (12), 3329–3330.

Hussein, A.M., 1993. Chemotherapy-induced alopecia: new developments. Southern Medical Journal 86 (5), 489–496.

Hussein, A.M., 1995. Protection against cytosine arabinoside-induced alopecia by minoxidil in a rat animal model, in mice. The Journal of Investigative Dermatology 34 (7), 470–473.

Hussein, A.M., Jimenez, J.J., McCall, C.A., Yunis, A.A., 1990. Protection from chemotherapy-induced alopecia in a rat model. Science 249 (4976), 1564–1566.

Hussein, A.M., Stuart, A., Peters, W.P., 1995. Protection against chemotherapy-induced alopecia by cyclosporin A in the newborn rat animal model. Dermatology 190 (3), 192–196.

Imai, Y., Matsushima, Y., Sugimura, T., Terada, M., 1991. A simple and rapid method for generating a deletion by PCR. Nucleic Acids Research 19 (10), 2785.

Jankovic, S.M., Jankovic, S.V., 1998. The control of hair growth. Dermatology Online Journal 4 (1), 2.

Jimenez, J.J., Yunis, A.A., 1992a. Protection from 1-beta-D-arabinofuranosylcytosine-induced alopecia by epidermal growth factor and fibroblast growth factor in the rat model. Cancer Research 52 (2), 413–415.

Jimenez, J.J., Yunis, A.A., 1992b. Protection from chemotherapy-induced alopecia by 1,25-dihydroxyvitamin D3. Cancer Research 52 (18), 5123–5125.

Jimenez, J.J., Huang, H.S., Yunis, A.A., 1992a. Treatment with ImuVert/*N*-acetylcysteine protects rats from cyclophosphamide/cytarabine-induced alopecia. Cancer Investigation 10 (4), 271–276.

Jimenez, J.J., Sawaya, M.E., Yunis, A.A., 1992b. Interleukin 1 protects hair follicles from cytarabine (ARA-C)-induced toxicity in vivo and in vitro. The FASEB Journal 6 (3), 911–913.

Kashio, A., Sakamoto, T., Suzukawa, K., Asoh, S., Ohta, S., Yamasoba, T., 2007. A protein derived from the fusion of TAT peptide and FNK, a Bcl-x(L) derivative, prevents cochlear hair cell death from aminoglycoside ototoxicity in vivo. Journal of Neuroscience Research 85 (7), 1403–1412.

Kim, R., Emi, M., Tanabe, K., Uchida, Y., Arihiro, K., 2006. The role of apoptotic or nonapoptotic cell death in determining cellular response to anticancer treatment. European Journal of Surgical Oncology 32 (3), 269–277.

Malkinson, F.D., Geng, L., Hanson, W.R., 1993. Prostaglandins protect against murine hair injury produced by ionizing radiation or doxorubicin. The Journal of Investigative Dermatology 101 (1 Suppl), 135S–137S.

Mitchell, D.J., Kim, D.T., Steinman, L., Fathman, C.G., Rothbard, J.B., 2000. Polyarginine enters cells more efficiently than other polycationic homopolymers. The Journal of Peptide Research 56 (5), 318–325.

Nagai, S., Asoh, S., Kobayashi, Y., Shidara, Y., Mori, T., Suzuki, M., Moriyama, Y., Ohta, S., 2007. Protection of hepatic cells from apoptosis induced by ischemia/reperfusion injury by protein therapeutics. Hepatology Research 37 (2), 133–142.

Ozaki, D., Sudo, K., Asoh, S., Yamagata, K., Ito, H., Ohta, S., 2004. Transduction of anti-apoptotic proteins into chondrocytes in cartilage slice culture. Biochemical and Biophysical Research Communications 313 (3), 522–527.

Park, J., Ryu, J., Park, J., Ryu, J., Jin, L.H., Bahn, J.H., Kim, J.A., Yoon, C.S., Kim, D.W., Han, K.H., Eum, W.S., Kwon, H.Y., Kang, T.C., Won, M.H., Kang, J.H., Cho, S.W., Choi, S.Y., 2002a. 9-polylysine protein transduction domain: enhanced penetration efficiency of superoxide dismutase into mammalian cells and skin. Molecules and Cells 13 (2), 202–208.

Park, J., Ryu, J., Kim, K.A., Lee, H.J., Bahn, J.H., Han, K., Choi, E.Y., Lee, K.S., Kwon, H.Y., Choi, S.Y., 2002b. Mutational analysis of a human immunodeficiency virus type 1 Tat protein transduction domain which is required for delivery of an exogenous protein into mammalian cells. The Journal of General Virology 83 (Pt 5), 1173–1181.

Paus, R., Handjiski, B., Eichmuller, S., Czarnetzki, B.M., 1994. Chemotherapy-induced alopecia in mice. Induction by cyclophosphamide, inhibition by cyclosporine A, and modulation by dexamethasone. The American Journal of Pathology 144 (4), 719–734.

Paus, R., Schilli, M.B., Handjiski, B., Menrad, A., Henz, B.M., Plonka, P., 1996. Topical calcitriol enhances normal hair regrowth but does not prevent chemotherapy-induced alopecia in mice. Cancer Research 56 (19), 4438–4443.

Ryser, H.J., 1968. Uptake of protein by mammalian cells: an underdeveloped area. The penetration of foreign proteins into mammalian cells can be measured and their functions explored. Science 159 (813), 390–396.

Sato, N., Leopold, P.L., Crystal, R.G., 2001. Effect of adenovirus-mediated expression of Sonic hedgehog gene on hair regrowth in mice with chemotherapy-induced alopecia. Journal of the National Cancer Institute 93 (24), 1858–1864.

Schilli, M.B., Paus, R., Menrad, A., 1998. Reduction of intrafollicular apoptosis in chemotherapy-induced alopecia by topical calcitriol-analogs. The Journal Investigative Dermatology 111 (4), 598–604.

Selleri, S., Arnaboldi, F., Vizzotto, L., Balsari, A., Rumio, C., 2004. Epithelium–mesenchyme compartment interaction and oncosis on chemotherapy-induced hair damage. Laboratory Investigation 84 (11), 1404–1417.

Sharov, A.A., Li, G.Z., Palkina, T.N., Sharova, T.Y., Gilchrest, B.A., Botchkarev, V.A., 2003. Fas and *c*-kit are involved in the control of hair follicle melanocyte apoptosis and migration in chemotherapy-induced hair loss. The Journal Investigative Dermatology 120 (1), 27–35.

Sharov, A.A., Siebenhaar, F., Sharova, T.Y., Botchkareva, N.V., Gilchrest, B.A., Botchkarev, V.A., 2004. Fas signaling is involved in the control of hair follicle response to chemotherapy. Cancer Research 64 (17), 6266–6270.

Shiraiwa, N., Inohara, N., Okada, S., Yuzaki, M., Shoji, S., Ohta, S., 1996. An additional form of rat Bcl-x, Bcl-xbeta, generated by an unspliced RNA, promotes apoptosis in promyeloid cells. The Journal of Biological Chemistry 271 (22), 13258–13265.

Snyder, E.L., Dowdy, S.F., 2005. Recent advances in the use of protein transduction domains for the delivery of peptides, proteins and nucleic acids in vivo. Expert Opinion on Drug Delivery 2 (1), 43–51.

Sordet, O., Khan, Q.A., Kohn, K.W., Pommier, Y., 2003. Apoptosis induced by topoisomerase inhibitors. Current Medical Chemistry Anticancer Agents 3 (4), 271–290.

Sordet, O., Khan, Q.A., Pommier, Y., 2004. Apoptotic topoisomerase I-DNA complexes induced by oxygen radicals and mitochondrial dysfunction. Cell Cycle 3 (9), 1095–1097.

Sredni, B., Xu, R.H., Albeck, M., Gafter, U., Gal, R., Shani, A., Tichler, T., Shapira, J., Bruderman, I., Catane, R., Kaufman, B., Whisnant, J.K., Mettinger, K.L., Kalechman, Y., 1996. The protective role of the immunomodulator AS101 against chemotherapy-induced alopecia studies on human and animal models. International Journal of Cancer 65 (1), 97–103.

Sudo, K., Asoh, S., Ohsawa, I., Ozaki, D., Yamagata, K., Ito, H., Ohta, S., 2005. The anti-cell death FNK protein protects cells from death induced by freezing and thawing. Biochemical and Biophysical Research Communications 330 (3), 850–856.

Suzuki, T., Futaki, S., Niwa, M., Tanaka, S., Ueda, K., Sugiura, Y., 2002. Possible existence of common internalization mechanisms among arginine-rich peptides. The Journal of Biological Chemistry 277 (4), 2437–2443.

Tara, S., Miyamoto, M., Asoh, S., Ishii, N., Yasutake, M., Takagi, G., Takano, T., Ohta, S., 2007. Transduction of the anti-apoptotic PTD-FNK protein improves the efficiency of transplantation of bone marrow mononuclear cells. Journal of Molecular and Cellular Cardiology 42 (3), 489–497.

Tsuda, T., Ohmori, Y., Muramatsu, H., Hosaka, Y., Takiguchi, K., Saitoh, F., Kato, K., Nakayama, K., Nakamura, N., Nagata, S., Mochizuki, H., 2001. Inhibitory effect of M50054, a novel inhibitor of apoptosis, on anti-Fas-antibody-induced hepatitis and chemotherapy-induced alopecia. European Journal of Pharmacology 433 (1), 37–45.

Tsuruki, T., Yoshikawa, M., 2005. Anti-alopecia effect of Gly-Leu-Phe, an immunostimulating peptide derived from alpha-lactalbumin. Bioscience, Biotechnology, and Biochemistry 69 (8), 1633–1635.

Tsuruki, T., Yoshikawa, M., 2006. Orally administered FPRL1 receptor agonist peptide MMK-1 inhibits etoposide-induced alopecia by a mechanism different from intraperitoneally administered MMK-1. Peptides 27 (4), 820–825.

Tsuruki, T., Takahata, K., Yoshikawa, M., 2005. Anti-alopecia mechanisms of soymetide-4, an immunostimulating peptide derived from soy beta-conglycinin. Peptides 26 (5), 707–711.

Veach, S.R., Schein, P.S., 1997. Supportive Care of Anon-hematologic Complications of Cytotoxic Therapy. In: Sweetnham, J.W., Williams, C. (Eds.), Supportive Care of the Cancer Patient. Arnold, New York, pp. 42–73.

Wang, J., Lu, Z., Au, J.L., 2006. Protection against chemotherapy-induced alopecia. Pharmaceutical Research 23 (11), 2505–2514.

Wender, P.A., Mitchell, D.J., Pattabiraman, K., Pelkey, E.T., Steinman, L., Rothbard, J.B., 2000. The design, synthesis, and evaluation of molecules that enable or enhance cellular uptake: peptoid molecular transporters. Proceeding of the National Academy of Sciences of the United States of America 97 (24), 13003–13008.

Available online at www.sciencedirect.com
ScienceDirect
Advanced Drug Delivery Reviews 60 (2008) 499–516
Advanced DRUG DELIVERY Reviews
www.elsevier.com/locate/addr

PTD-mediated delivery of anti-cell death proteins/peptides and therapeutic enzymes ☆

Sadamitsu Asoh *, Shigeo Ohta

Department of Biochemistry and Cell Biology, Institute of Development and Aging Sciences, Graduate School of Medicine, Nippon Medical School, 1-396, Kosugi-cho, Nakahara-ku, Kawasaki-city, Kanagawa 211-8533, Japan

Received 14 August 2007; accepted 12 September 2007
Available online 13 November 2007

Abstract

Millions of unnecessary cells are removed from our body everyday by apoptosis to ensure our survivals. Apoptosis is a highly coordinated process. Failure in apoptotic regulation results in disease. A large number of studies have demonstrated that accelerated apoptosis is involved in degenerative diseases, ischemic injuries, immunodeficiency and infertility. These studies have also revealed the molecular mechanisms of apoptosis signal transduction to provide therapeutic targets. On the other hand, protein transduction technology has been developed to deliver full-length proteins to various tissues including the brain. So far, many studies have shown that *in vivo* delivery of therapeutic proteins/peptides, including anti-apoptotic proteins, an anti-oxidant enzyme, a neuroprotectant, enzymes involved in purine or tyrosine metabolism, caspase inhibitors, c-Jun N-terminal kinase inhibitors and an NF-κB inhibitor, by protein transduction technology mitigates various diseases in animal models.

Keywords: Apoptosis; Bcl-2 family; Enzyme replacement; Ischemia/reperfusion injury; Necrosis; Neurodegenerative diseases; Peptide inhibitors; Protein therapy

Contents

☆ This review is part of the *Advanced Drug Delivery Reviews* theme issue on "Membrane Permeable Peptide Vectors: Chemistry and Functional Design for the Therapeutic Applications".

* Corresponding author. Tel.: +81 44 733 1859; fax: +81 44 733-9268.
E-mail address: sada@nms.ac.jp (S. Asoh).

0169-409X/$ - see front matter © 2007 Elsevier B.V. All rights reserved.
doi:10.1016/j.addr.2007.09.011